GJB1 MUTATION SCREENING AND *IN VITRO* INVESTIGATION OF ITS UPSTREAM MUTATIONS

by

Oğuz Arı

B.S., Molecular Biology and Genetics, Boğaziçi University, 2014

Submitted to the Institute for Graduate Studies in
Science and Engineering in partial fulfillment of
the requirements for the degree of
Master of Science

Graduate Program in Molecular Biology and Genetics
Boğaziçi University
2017

GJB1 MUTATION SCREENING AND *IN VITRO* INVESTIGATION OF ITS UPSTREAM MUTATIONS

APPROVED BY:

Prof. Esra Battaloğlu . . . .
(Thesis Supervisor)

Prof. Hande Çağlayan . . . .

Prof. Eda Tahir Turanlı . . . .

DATE OF APPROVAL: 13.04.2017

To my family and friends...

ACKNOWLEDGEMENTS

First and foremost, I would like to express my sincere gratitude to my thesis supervisor Prof. Esra Battaloğlu for her valuable guidance, criticisim and encouragement throughout the study. I would like to thank my thesis committee members, Assoc. Prof. Eda Turanlı and Prof. Hande Çağlayan for devoting their time to evaluate this thesis.

I am grateful to Aslı Uğurlu for cell culture experiments and İzzet Akiva for luciferase assays. I would like to express my special thanks to my lab members Burçak Özeş, Ayşe Candayan, Cansu Küey, Elif Begüm Gökerküçük and Büşra Şimşek for teaching me all the laboratory basics, as well as giving me useful hints about the methods.

I would like to thank all Teras lab members; Mahmut Can Hız, Emirhan Taşöz, Neslihan Zöhrap, Burcu Ersoy, Ceren Saygı, Dilvin Yıldırım for creating such a warm laboratory environment and also my friends Özen Kaya, Büşra Çoban, Esra Yıldız, Mehmet Can Demirler, Ali İşbilir, Çağrı Çevrim, Nalan Yıldız and Metin Özdemir at the department for their constant moral support. Harun Niron, İsmail Tuğberk Kaya, Serdar Çapar, Burak Bali, Nazmiye Özkan, Buğra Aktan, Onurcan Albayrak and Hasan Burak Tavşanoğlu deserve special thanks. I also thank to all other members of MBG for their contribution to my graduate experience.

The last but not the least, I would like to express my deepest appreciation to my beloved family for their love, motivation and support throughout my life.

I am grateful to The Scientific and Technological Research Council of Turkey (TÜBİTAK – 114S725) for financial support. I would also like to thank all clinicians and patients who participated in this project.

This study was supported by Boğaziçi University Research Fund (BAP 11280).

ABSTRACT

GJB1 MUTATION SCREENING AND *IN VITRO* INVESTIGATION OF ITS UPSTREAM MUTATIONS

Charcot-Marie-Tooth Type 1X (CMTX1) is the X chromosome linked form of the disease and caused by mutations in the gap junction protein 1 (*GJB1*) gene. This gene is the second most commonly mutated gene in all CMT forms after PMP22 gene duplication and covers 10% of all CMT cases. More than 400 different mutations have been identified in all regions of this gene, up to date. All types of mutations such as missense, nonsense, splice site mutations, small insertions, deletions leading to formation of truncated protein were reported and some rare patients have whole gene deletions. Variants in 5' promoter region were reported in a few patients. These variants are expected to reduce the gene expression level and cause loss of function. In previous years, two novel upstream mutations (c.-541A> G and c.-528T> C) were identified in our lab. In this study, we screened 50 patients from our Turkish CMT cohort for *GJB1* mutations using PCR and direct sequencing strategy. Eight different variants were identified in *GJB1* including three 5' UTR variants. Among them, two coding region and one upstream variants were novel mutations. In the second part, we investigated the effects of 5' mutations that were identified in our lab, using luciferase reporter gene assay by expressing these *GJB1* upstream variants (c.-18A>G, c.-541A> G, c.-528T> C and c.-713G>A) in HEK293T cells. The c.-541A> G and c.-528T> C mutations are located inside the promoter of GJB1 gene and caused significant reduction in gene expression level providing evidence for the loss of function effect of these variants. The c.-18A>G variant was also shown to cause a slight decrease in gene expression. It is located in a splice site of the gene and possibly responsible for abnormal protein production. Lastly, c.-713G>A which was previously reported as a polymorphism caused no significant effect on luciferase expression. This study contributed to molecular diagnosis of CMTX1, described a common upstream variant in our CMT population, and demonstrated reduced gene expression effect for three novel upstream variants.

ÖZET

GJB1 MUTASYON TARAMASI VE PROMOTÖR MUTASYONLARININ GEN ANLATIMINA ETKİLERİNİN İNCELENMESİ

Charcot-Marie-Tooth Tip 1X (CMTX1), CMT hastalığının X kromozomuna bağlı seyreden tipidir ve gap junction protein 1 (*GJB1*) gen mutasyonlarından kaynaklanır. *GJB1* geni tüm CMT tipleri içinde, PMP22 gen duplikasyonundan sonra, en sık mutasyon görülen ikinci gendir ve hastaların %10'unu kapsar. Bugüne kadar yaklaşık 400 farklı *GJB1* gen mutasyonu tanımlanmıştır. Gende yanlış anlam ve anlamsız mutasyonlar, küçük delesyon ve insersiyonlar olabileceği gibi tüm genin silindiği hastalar da belirlenmiştir. Genin 5' ucundaki promotör bölgesinde ise çok az sayıda mutasyon tanımlanmıştır; protein dizisine etki etmeseler de genin anlatım düzeyini düşürerek işlev kaybına neden oldukları savlanmaktadır. Önceki yıllarda, laboratuvarımızda iki yeni promotör mutasyonu (c.-541A>G ve c.-528T>C) belirlenmiştir. Bu çalışmada ise, toplumumuz CMT hastaları arasından seçilen 50 hastada yeni mutasyonların belirlenmesi amacıyla *GJB1* geni tarandı ve üçü 5' düzenleyici bölgede toplam sekiz farklı varyant saptandı. Bunlardan, üçü daha önce rapor edilmemiş yeni mutasyonlardır. İkinci bölümde, laboratuvarımızda tanımlanan dört düzenleyici bölge varyantının gen anlatımına etkileri lusiferaz raportör geni aracılığıyla araştırıldı. Bu analizde varyant (c.-18A>G, c.-541A>G, c.-528T>C ve c.-713G>A) içeren promotör dizileri altında lüsirefaz geni içeren plazmidler HEK293T hücrelerine aktarılarak lüsiferaz gen anlatımı sağlandı. Promotör bölgesinde yer aldığı bilinen c.-541A>G ve c.-528T> C varyantlarının, lüsiferaz anlatımında anlamlı düşüşe neden oldukları gösterilerek CMT fenotipinden sorumlu olabilecekleri gösterildi. Aynı zamanda, c.-18A>G varyantının da gen anlatımında azalmaya neden olduğu belirlendi. Söz konusu varyant genin kırpılma bölgesinde bulunduğundan bozuk protein üretiminden sorumlu olabileceği öngörülmektedir. Son olarak, c.-713G>A varyantının, literatürle uyumlu olarak, gen anlatımı üzerinde bir etkiye neden olmadığı gösterildi. Bu çalışma ile CMTX1 moleküler tanısına katkıda bulunulmuş, CMT hastalarında yaygın bir varyant tanımlanmış ve üç yeni promotör varyantının *GJB1* anlatımını düşürdüğü gösterilmiştir.

TABLE OF CONTENTS

ACKNOWLEDGEMENTS iv

ABSTRACT v

ÖZET vi

LIST OF FIGURES xi

LIST OF TABLES xiv

LIST OF ACRONYMS/ABBREVIATIONS xvi

1. INTRODUCTION 1

1.1. Charcot-Marie-Tooth Disease 1

1.2. X-Linked Charcot-Marie-Tooth Disease (CMTX) 3

1.3. Connexin-32 Protein 4

1.4. Regulation of *GJB1* Gene Expression 7

1.4.1. Mutations in the Coding Region of *GJB1* Gene 8

1.4.2. Mutations in the 5’UTR of *GJB1* Gene 9

2. PURPOSE 12

3. MATERIALS 13

3.1. Subjects 13

3.2. Chemicals 13

3.3. General Kits, Enzymes, and Reagents 13

3.4. Biological Materials ... 14
3.4.1. Bacterial Strain ... 14
3.4.2. Mammalian Cell Line ... 14
3.5. Buffers and Solutions ... 15
3.5.1. DNA Extraction from Peripheral Blood ... 15
3.5.2. Polymerase Chain Reaction (PCR) ... 15
3.5.3. Restriction Enzyme Analysis ... 16
3.5.4. Agarose Gel Electrophoresis ... 16
3.5.5. Bacterial Culture Solutions and Antibiotics ... 17
3.5.6. Cell Culture ... 18
3.6. Nucleic Acids ... 18
3.6.1. Plasmids ... 18
3.6.2. Oligonucleotides ... 19
3.7. Disposable Labware ... 21
3.8. General Equipment ... 21
4. METHODS ... 23
4.1. DNA Extraction from Peripheral Blood ... 23
4.2. Quantitative Analysis of Purified DNA ... 23
4.3. Mutation Analysis ... 24

4.3.1. Mutational Analysis of CDS and 5’ UTR of *GJB1* by PCR-Direct Sequencing 24
4.4. Molecular Cloning 25
4.4.1. PCR Amplification of Insert DNA 25
4.4.2. Restriction Digestion of Vector 26
4.4.3. Agarose Gel Electrophoresis 26
4.4.4. PCR Purification 27
4.4.5. Gibson Assembly Cloning 27
4.4.6. Transformation of Competent Cells 28
4.4.7. Colony PCR 28
4.4.8. Plasmid DNA Purification and Sequencing 29
4.4.9. Phenol-Chloroform and Ethanol Precipitation 29
4.5. Site-Directed Mutagenesis 30
4.5.1. Linearization of Plasmid by PCR 30
4.5.2. Non-Radioactive Phosphorylation with T4 PNK 30
4.5.3. Ligation of Plasmid 31
4.6. Cell Culture Experiments 31
4.6.1. Maintenance of HEK293T Cells 31
4.6.2. Freezing of HEK293T Cells 32
4.6.3. Thawing of HEK293T Cells 32

4.6.4. Transfection of HEK293T Cells ... 32

4.7. Luciferase Reporter Assay ... 33

5. RESULTS ... 35

5.1. Mutational Analysis ... 35

5.1.1. Mutational Analysis of *GJB1* coding sequence ... 35

5.1.2. Mutational Analysis of 5’UTR of *GJB1* ... 40

5.2. Functional Analysis of 5’UTR Variants ... 42

5.2.1. Construction of Plasmids ... 42

5.2.2. Purification of Plasmids ... 44

5.2.3. Generation of c.-541A>G Variant by Site-Directed Mutagenesis ... 45

5.3. Co-transfection of HEK293T Cells and Luciferase Assay ... 47

6. DISCUSSION ... 50

6.1. Mutation Analysis of *GJB1* ... 50

6.1.1. Mutations on CDS of *GJB1* ... 50

6.1.2. Mutations in 5’UTR of *GJB1* and Their Effects on Gene Expression ... 52

7. CONCLUSION ... 56

REFERENCES ... 57

APPENDIX A: PLASMID MAPS ... 66

APPENDIX B: MAP OF SPLICE SITE SEQUENCES ... 69

APPENDIX C: LUCIFERASE ASSAY DATA ... 70

LIST OF FIGURES

Figure 1.1. Deformities in hands and knees in an affected patient. 1

Figure 1.2. Genetic classification of CMT. 2

Figure 1.3. Oligomerization of connexins 6

Figure 1.4. Diagram of *GJB1* gene and different transcripts. 7

Figure 1.5. Diagram of Cx32 protein showing amino acid changes. 8

Figure 1.6. Pedigree of family P232. 10

Figure 1.7. Pedigree of family P158. 10

Figure 1.8. Pedigree of family P727. 11

Figure 5.1. Chromatograms for P1021, 1186, P1020 and control. 36

Figure 5.2. Conservation of Isoleucine at 127th amino acid position among mammalian species. 37

Figure 5.3. Chromatograms for P1113, P553 and control. 37

Figure 5.4. Chromatograms for P763 and control. 38

Figure 5.5. Chromatograms for P1027-3 and control. 38

Figure 5.6. Conservation of Cysteine at 168th amino acid position among mammalian species. 39

Figure 5.7. Chromatograms for P711 and control. 39

Figure 5.8. Chromatograms for P980, P1256 and control. 40

Figure 5.9 Chromatograms for P9374 and control. 41

Figure 5.10. Agarose gel image of PCR amplified *GJB1*-5'UTR fragments. 43

Figure 5.11. Agarose gel image of colony PCR results. 43

Figure 5.12. Agarose gel image of colony PCR results. 44

Figure 5.13. Agarose gel image of purified plasmids. 44

Figure 5.14. The map of pGL2-GJB1 vector. 45

Figure 5.15. Agarose gel image of linearized wild type plasmids by PCR using primers containing c.-541A>G variant. 46

Figure 5.16. Agarose gel image of colony PCR results containing c.-541A>G variant. 46

Figure 5.17. Agarose gel image of purified plasmids containing c.-541A>G variant. 47

Figure 5.18. Functional impact of the variants in the *GJB1*-5'UTR on luciferase expression and its activity. 48

Figure 6.1. Diagram of *GJB1* and upstream mutations that were investigated in this study. 53

Figure 6.2. In silico analysis of c.-18A>G. 54

Figure 6.3. Generated splice site motif. 54

Figure A.1. Restriction map and Multiple Cloning Site (MCS) of pGL2-basic vector which is used to generate pGL2-GJB1 plasmid. 66

Figure A.2. Map of SOX10 expression plasmid used to provide SOX10 transcription factor protein in HEK293T cells. 67

Figure A.3. Map of pRL-SV40 Renilla Luciferase plasmid that used as internal control in luciferase assays..68

Figure B.1. Transcription template sequence and splice site region of *GJB1*. 69

Figure B.2. Splice site region of luciferase plasmid containing upstream sequence of *GJB1*. 69

Figure C.1. Signals for firefly and renilla luciferase luminescence for different variants. . 70

LIST OF TABLES

Table 1.1. Connexin-associated diseases and corresponding connexin proteins and genes. . 5

Table 3.1. List of kits, enzymes, and reagents. 13

Table 3.2. Buffers and chemicals that were used for DNA extraction from peripheral blood. 15

Table 3.3. The buffer and the chemicals used for PCR. 15

Table 3.4. Buffer that used for restriction digestion. 16

Table 3.5. Ingredients that are used for Agarose Gel Electrophoresis 16

Table 3.6. Solutions and Antibiotics used for the growth and maintenance of bacterial cultures. 17

Table 3.7. Buffers and solutions used in cell culture. 18

Table 3.8. Sequence of the primers used for exon amplification of *GJB1* for PCR and Sanger sequencing. 19

Table 3.9. Sequence of the primers used for 5’UTR amplification of *GJB1*. 19

Table 3.10. Sequence of the primers used to linearize pGL2-GJB1 plasmid to generate c.-541A>G variant by site-directed mutagenesis. 20

Table 3.11. Sequence of the primers used for colony PCR. 20

Table 3.12. Sequence of the primers used to amplify insert DNA for Gibson Assembly. . . 20

Table 3.13. List of disposable labware used in this study. 21

Table 3.14. Equipment used during this study. 21

Table 4.1. PCR for CDS and 5’UTR amplification of *GJB1*. 24

Table 4.2. Conditions of PCR for CDS and 5’UTR of *GJB1*. 25

Table 4.3. PCR protocol using the Phusion High-Fidelity DNA Polymerase. 26

Table 4.4. Ingredients for PCR using the Phusion High-Fidelity DNA Polymerase. 26

Table 4.5. Ingredients for Gibson Assembly reaction. 28

Table 4.6. Conditions of Colony PCR. 28

Table 4.7. Ingredients for phosphorylation by T4 PNK. 30

Table 4.8. Ingredients for ligation reaction by T4 DNA Ligase. 31

Table 4.9. Plasmids used in transfection experiments. 33

Table 5.1. The mutations and the clinical data of the patients. 41

Table 5.2. Patients that used for amplification of insert DNA and corresponding variants.43

LIST OF ACRONYMS/ABBREVIATIONS

AD	Autosomal Dominant
Amp	Ampicillin
AR	Autosomal Recessive
ATP	Adenosine Triphosphate
bp	Base Pair
$CaCl_2$	Calcium Chloride
cAMP	Cyclic Adenosine Monophospate
CMT	Charcot Marie Tooth
CNS	Central Nervous System
Cx26	Connexin-26
Cx30	Connexin-30
Cx31	Connexin-31
Cx32	Connexin-32
Cx40	Connexin-40
Cx43	Connexin-43
Cx46	Connexin-46
Cx47	Connexin-47
Cx50	Connexin-50
CNS	Central Nervous System
CO_2	Carbon Dioxide
DMEM	Dulbecco's Modified Eagle Medium
DMSO	Dimethyl Sulfoxide
DNA	Deoxyribonucleic Acid
EDTA	Ethylenediaminetetraacetic Acid
ER	Endoplasmic Reticulum
FBS	Fetal Bovine Serum
ESS	Exonic Splicing Silencer
EtOH	Ethanol
GJA1	Gap junction protein, alpha 1

GJA3	Gap junction protein, alpha 3
GJA5	Gap junction protein, alpha 5
GJA8	Gap junction protein, alpha 8
GJA12	Gap junction protein, alpha 12
GJA3	Gap junction protein, alpha 3
GJA5	Gap junction protein, alpha 5
GJA8	Gap junction protein, alpha 8
GJB1	Gap junction protein beta-1
GJB2	Gap junction protein beta-2
GJB3	Gap junction protein beta-3
GJB4	Gap junction protein beta-4
GJB6	Gap junction protein beta-6
GJC2	Gap junction protein gamma-2
HCl	Hydrochloric Acid
HEK293T	Human Embryonic Kidney 293T
hrs	Hours
KCl	Potassium chloride
het	Heterozygous
HGMD	Human Genome Mutation Database
HSMN	Hereditary Motor and Sensory Neuropathy
HNPP	Hereditary Neuropathy with Liability to Pressure Palsy
hom	Homozygous
IP_3	Inositol trisphosphate
kb	Kilobase
kDa	Kilodalton
LB	Luria Broth
Luc	Luciferase
mg	Miligram
$MgCl_2$	Magnesium Chloride
Min	Minute
ml	Mililiter
mM	Milimolar
NA	Not available

Na_2EDTA	Disodium Ethylenediamine Tetraacetate
NaCl	Sodium Chloride
NaOH	Sodium hydroxide
NCBI	National Center for Biotechnology Information
NCV	Nerve conduction velocity
ng	Nanogram
nm	Nanometer
ORF	Open Reading Frame
PBS	Phosphate Buffered Saline
PCR	Polymerase Chain Reaction
PNK	Polynucleotide Kinase
RBC	Red Blood Cell
RNA	Ribonucleic Acid
rpm	Rotations Per Minute
SDS	Sodium Dodecyl Sulfate
SOC	Super optimal catabolite repressed broth
Sox10	SRY (sex determining region Y) Box 10
TBE	Tris-Borate-EDTA
TE	Tris-EDTA
Temp	Temperature
UTR	Untranslated Region
v/v	Volume to volume
w/v	Weight to volume
WT	Wild-type

1. INTRODUCTION

1.1. Charcot-Marie-Tooth Disease

Charcot Marie Tooth (CMT), also known as Hereditary Motor and Sensory Neuropathy (HMSN), is a hereditary disease affecting motor and sensory nerves. It was named after three neurologists who described the disease in 1886: Jean-Martin Charcot, Pierre Marie and Howard Henry Tooth (Charcot and Marie, 1886; Tooth, 1886). Patients with this disease generally have symptoms such as muscle weakness, loss of sense and movement in the hands and wrists, and deformities in the feet (Figure 1.1).

Figure 1.1. Deformities in hands and knees in an affected patient (Hahn *et al*., 1990).

According to clinical and electrophysiological findings, CMT disease is classified as demyelinating, axonal, and intermediate (Berciano *et al*., 2011). 'Demyelinating' type is characterized by low nerve conduction velocity (NCV) due to defects in myelin forming Schwann cells. This type of neuropathy is known as CMT type 1 (CMT1). In 'Axonal' type of CMT, CMT type 2 (CMT2), NCV values are normal, however, muscle action potential is reduced since degeneration affects the axons of neurons. The third form of CMT is called 'intermediate' type since NCV values are moderate in between 25-45 m/s and both demyelination and axonal degeneration are observed (Reilly *et al*., 2011).

When CMT disease is genetically assessed, it is possible to see all types of Mendelian hereditary patterns. Although autosomal dominant form of the disease is responsible for the most of the cases, autosomal recessive and X chromosome linked types are also observed (Reilly *et al.*, 2011). In order to have an accurate classification of all CMT cases, both clinical and inheritance features should be taken into consideration.

The number of genes known to be responsible for CMT has increased to over 40 with the emergence of next generation sequencing technologies in recent years (Figure 1.2). Despite the use of this advanced technology to screen all these genes for mutations for genetic diagnosis, the cause of the disease remains unknown in about 30-35% of the patients (Saporta *et al*. 2011). This finding implicates that there are still many CMT genes remain to be identified. Another problem in genetic diagnosis of CMT patients is the presence of genetic and clinical heterogeneity that makes it difficult to establish a genotype/phenotype correlation (Reilly *et al*. 2011).

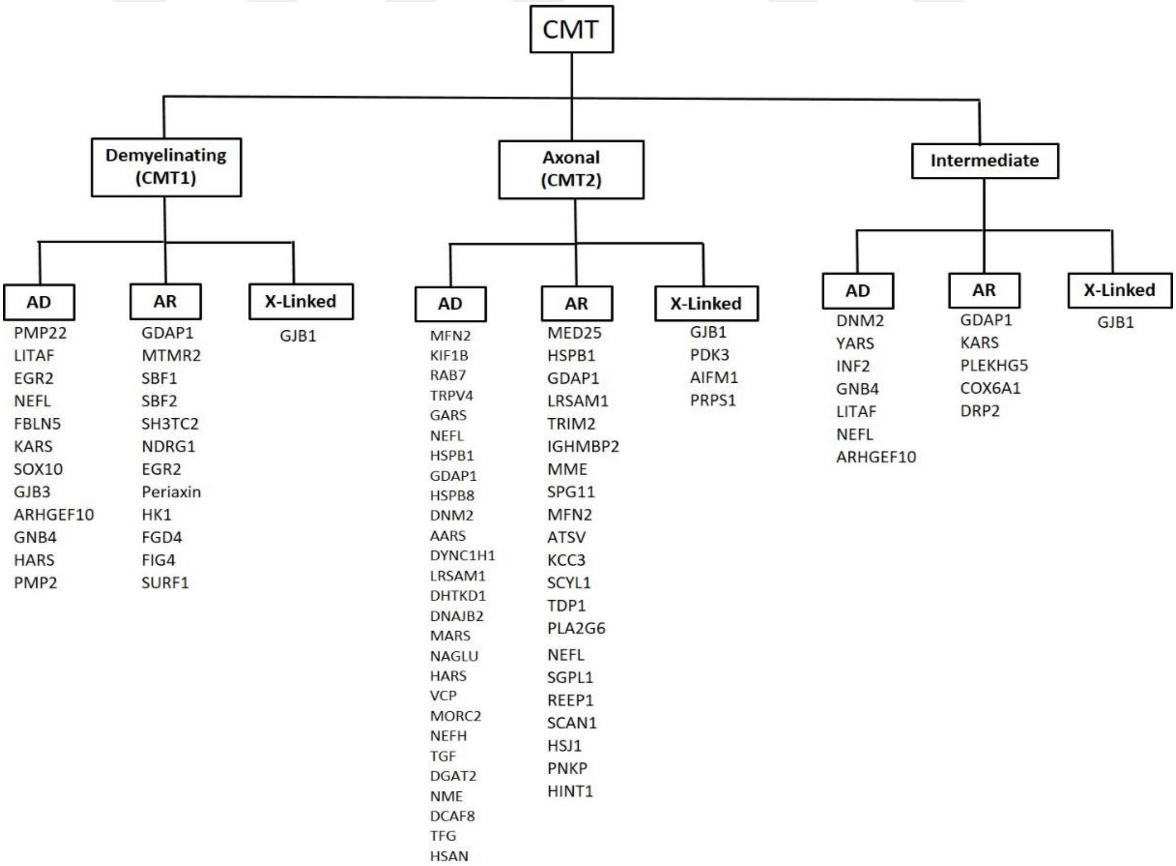

Figure 1.2. Genetic classification of CMT.

1.2. X-Linked Charcot-Marie-Tooth Disease (CMTX)

Charcot-Marie-Tooth Type 1X (CMTX1) is an X chromosome-mediated form of the CMT disease and originates from gap junction protein 1 (*GJB1*) gene mutations. After the *PMP22* gene duplication (CMT1A), CMTX1 is the second most frequent type and responsible for about 10% of the all CMT cases (Murphy *et al*., 2012; Saporta *et al*., 2011). Up to now, approximately 400 different *GJB1* gene mutations have been identified (Kleopa *et al*., 2014). These mutations are usually missense variants in the single protein coding exon of the gene. Nonsense mutations that lead to short protein formation, small deletions and insertions as well as whole gene deletions are also observed in CMTX1 patients (Ionasescu *et al*., 1996; Houlden *et al*., 2004). Very few mutations have been identified in the promoter region of the gene. It is argued that they cause loss of genetic expression by disrupting transcription factor binding sites on the promoter region of *GJB1* or altering the splicing process.

Patients with CMTX phenotype generally have homogenous symptoms but the age of onset and progression of the disease may differ even among the same family members depending on the genetic background. Studies conducted in large patient groups showed that walking difficulties and muscle weakness increased with age (Wang *et al*., 2015). Appearance of the same symptoms in both whole gene deleted patients and those with missense/nonsense mutations suggests that loss of protein function is the responsible genetic mechanism that causes the disease (Shy *et al*. 2007). As with other CMT types, progression is slow and begins with muscle weakness and atrophy in the distal leg muscles. Patients complain of frequent falls and buckling before 10 years of age (Kuntzer *et al*., 2003). Mostly males are affected as expected from X-linked inheritance. In addition, middle-aged females can also be affected due to random X chromosome inactivation (Murphy, Ovens *et al*., 2012).

CMT is a peripheral neuropathy, however, central nervous system can also be affected in CMTX1 patients. Accompanied by peripheral neuropathy, spasticity, cerebellar ataxia, and encephalopathy are reported in some patients (Kleopa *et al*., 2002; Paulson *et al*., 2002). In electrophysiological and clinical studies, it was shown that latencies of brainstem auditory evoked responses are delayed in most CMTX1 patients (Nicholson *et al*., 1998; Senderek *et al*., 1999) in addition to possible involvement of central visual and motor pathways (Bähr *et al*., 1999). Remarkably, these electrophysiological findings are not observed on the cases with *GJB1* gene deletions. Therefore, this findings can imply a gain of function effect for CNS manifestations in CMTX1 phenotype (Hahn *et al*., 2000).

1.3. Connexin-32 Protein

GJB1 gene encodes a 32 kDa protein called Connexin-32 (Cx32) that belongs to the family of gap junction proteins (Kumar and Gilula, 1986; Paul, 1986). It is a transmembrane protein and forms hemi-channels or connexons in the membrane as the other members of gap junction family. There are at least 20 different types of connexin proteins that function as transmembrane proteins in gap junctions (Sohl *et al*., 2003).

Connexons are hexamer structures that reside on the cell membrane. They are formed by oligomerization of six connexin proteins on Golgi apparatus or Endoplasmic Reticulum. One of those connexons in the cell membrane docks end-to-end with another connexon from opposing neighbouring cell in order to form a gap junction (Figure 1.3). The center of this channels is approximately 1.2 nm and provides ion and nutrient flow between the two cells. Through these connections, intercellular metabolic partnership, communication, buffering, electric current and growth control of the cells are accomplished (Goldberg *et al*., 2004).

Due to their important role in cell-to-cell interaction and communication, mutations in connexin genes cause a wide variety of disorders such as myelin-related diseases (CMT), skin disorders, hearing loss, congenital cataract, or more complex syndromes such as oculodendrodigital dysplasia (Pfenniger *et al*., 2011). It was shown that different mutations even in the same connexin gene may result in different disorders. For example, different mutations in Cx30 gene may cause either hearing loss, skin disease or Clouston syndrome (Table 1.1).

Table 1.1. Connexin-associated diseases and corresponding connexin proteins and genes (Pfenniger *et al.*, 2011).

Disease	**Inheritance pattern**	**Connexin Protein**	**Gene**
Oculodendrodigital dysplasia	AD/AR	Cx43	GJA1
Cardiovascular diseases			
Atrial fibrillation	AD/ND	Cx40	GJA5
Visceroatrial heterotaxia	AD	Cx43	GJA1
Cataract	AD	Cx46	GJA3
		Cx50	GJA8
Myelin-related diseases			
X-linked Charcot-Marie-Tooth disease	XR	Cx32	GJB1
Pelizaeus–Merzbacher-like disease	AR	Cx46-6/ Cx47	GJA12/ GJC2
Hearing loss (non-syndromic or associated with skin disorders)	AR/AD	Cx26	GJB2
		Cx30	GJB6
		Cx31	GJB3
Skin diseases	AD		
Keratitis ichthyosis deafness syndrome		Cx26	GJB2
		Cx30	GJB6
Vohwinkel syndrome		Cx26	GJB2
Clouston syndrome		Cx30	GJB6
Erythrokeratodermia variabilis		Cx30-3	GJB4
		Cx31	GJB3

Expression of connexin-32 protein initially starts on ER membrane. High level of connexin production leads to oligomerization in ERGIC (ER-Golgi Intermediate Compartment) sites (Koval, 2006). Connexon hemi-channels are subsequently transported through Golgi apparatus to the cell membrane where it forms complete gap junctions.

(Figure 1.3) Moreover, channels formed by different types of connexin proteins may form gap junction plaques in adjacent cell membranes (Segretain *et al*., 2004).

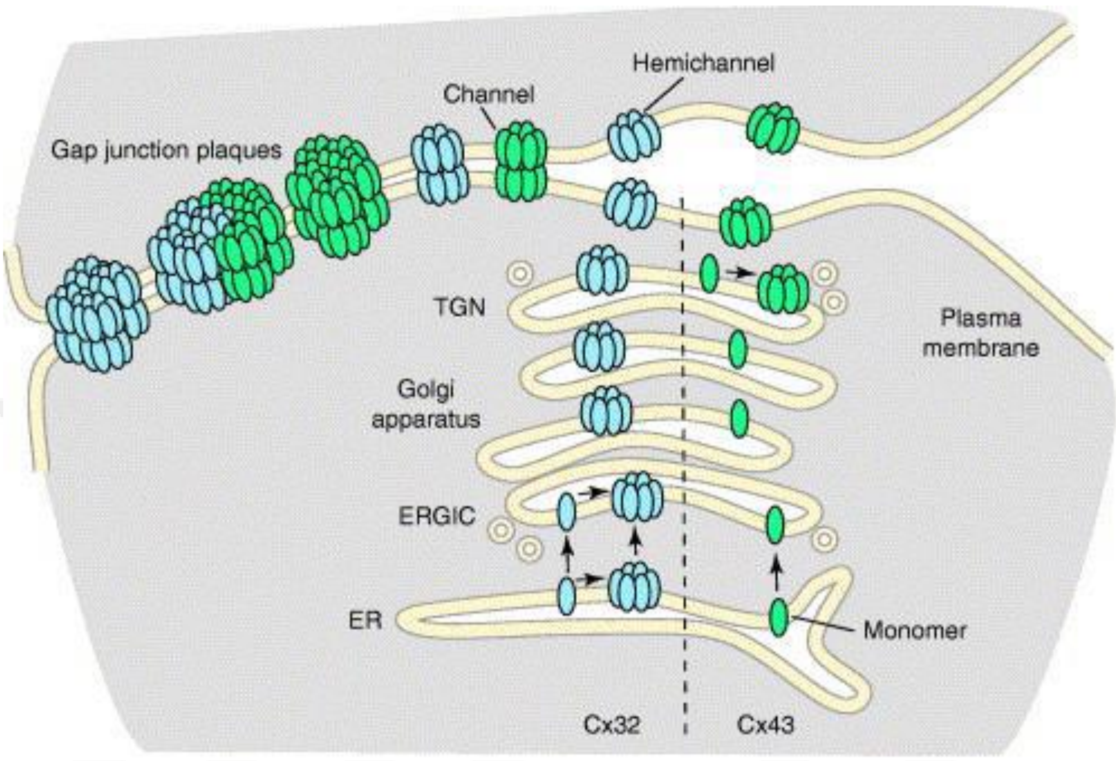

Figure 1.3. Oligomerization of connexins (Koval, 2006)

The association of the Cx32 protein with CMT disease is due to its expression in Schwann cells that form the myelin sheet in peripheral nerves (Orthmann-Murphy *et al*., 2007). On the other hand, it is known that the nerve cells wrapped with myelin are also affected in CMTX1 patients (Kleopa *et al*., 2011). Because of this, *GJB1* mutations are classified as ‘intermediate’ type of CMT. As such, patients with CMTX1 may have both low to medium NCV values due to demyelination and reduced axon potential caused by affected neurons. Studies have shown that nerve cells are affected before the initiation of Schwann cell degeneration, the number of neurofilaments increase, and their walls are narrowed (Kleopa *et al*., 2011). This differentiation suggests that the neuronal structure is impaired and cause axonal neuropathy by affecting axonal transport.

1.4. Regulation of *GJB1* Gene Expression

GJB1 is a 10,000 base pair long gene which consist of three promoters, an intron and two exons (Tsai *et al*., 2013). Exon 1 does not code for amino acids and removed by splicing process after transcription. *GJB1* gene encodes three different transcripts due to alternative use of its promoters. (Figure 1.4). It has three different promoter sites designated as P1, P2, and P3 in the 5' UTR of the gene (Neuhaus *et al*., 1995, 1996; Söhl *et al*., 1996, 2001). Each promoter is responsible for production of different transcripts in various cells and tissues. Nerve specific transcript of *GJB1* gene is mainly controlled by P2 promoter whereas transcription is initiated by P1 and/or P3 promoter in other cells such as liver, pancreas and embryonic stem cells. Neuronal cells in central nervous system (CNS) use both P1 and P2 promoters to produce connexin-32 protein.

The P2 promoter which regulates the expression of the *GJB1* gene in neurons contains two SOX10 transcription factor binding sites, designated as S1 and S2. In a healthy nerve cell, SOX10 protein binds to this transcription factor binding sites and initiate gene expression (Kuhlbrodt *et al*., 1998). Therefore, it is possible that sequence variants in S1 and S2 sites can reduce the general expression of the *GJB1* gene. In addition, variants at the junction of intron and exon 2 of *GJB1* gene may cause disruption in splicing while removing the non-coding exon 1 from the transcript.

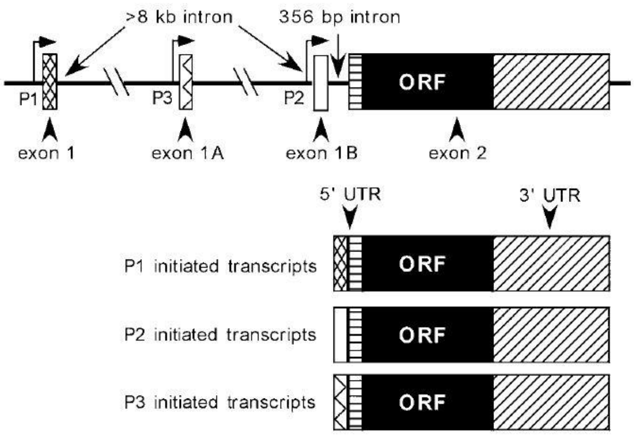

Figure 1.4. Diagram of *GJB1* gene and different transcripts. Different promoters are designated as P1, P2 and P3 (Scherer and Paul, 2004).

1.4.1. Mutations in the Coding Region of *GJB1* Gene

About 400 different *GJB1* gene mutations have been identified in CMT patients (Kleopa *et al* 2012). Those mutations may have various effects on cellular and molecular level (Figure 1.5). Most of these mutations are located in protein coding region and cause non-functional gap junction channels. For example, two mutations (S26L; M34T) in the coding region of *GJB1* were shown to cause reduced pore size in gap junctions (Oh *et al*., 1997) that may prevent transport of secondary messengers such as IP3, cAMP, and Ca^{2+}. On the other hand, it was reported that some mutations (S85C and F235C) may cause toxic gain-of-function effect in gap junctions (Liang *et al*., 2005; Abrams *et al*., 2002). These mutants lead to functional but 'leaky' hemi-channels that have increased opening time (Liang *et al*., 2005).

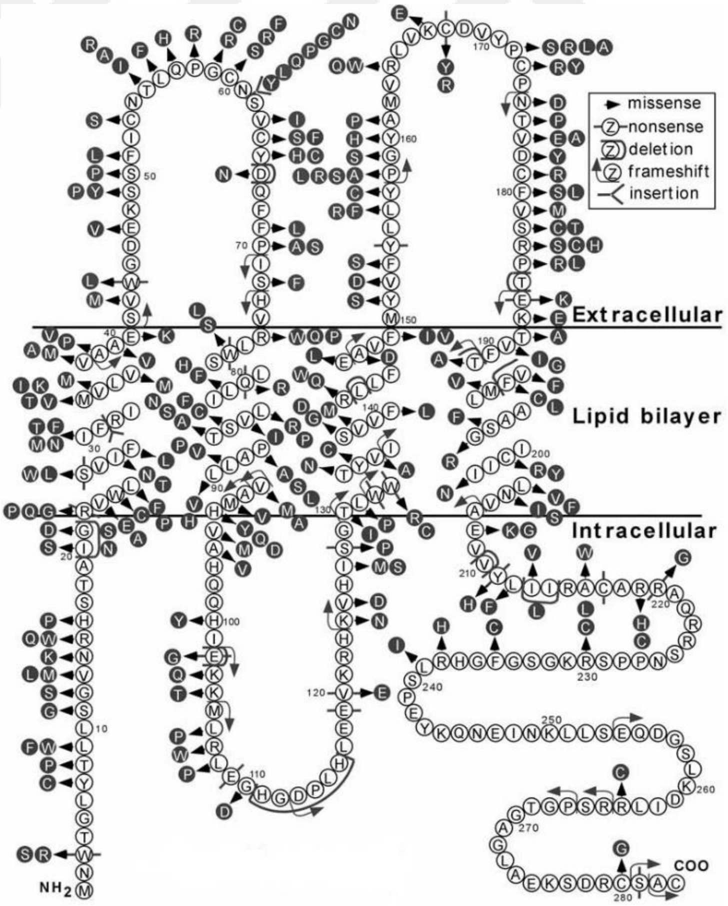

Figure 1.5. Diagram of Cx32 protein showing amino acid changes leading to CMT phenotype (Kleopa and Scherer, 2002).

Effect of a variant may not be predicted from its position as for R15Q and H94Q variants. These mutants were shown to form functional gap junctions, however, different transitions in the same amino acid positions (R15W; H94Y) result in non-functional channels. This finding implicates the importance of the nature of the mutation for the phenotype (Abrams *et al*., 2002).

1.4.2. Mutations in the 5'UTR of *GJB1* Gene

Mutations which are identified in the non-coding region of *GJB1* gene are observed rarely may be due to the fact that it is not screened for mutations in most studies. The effect of these mutations on gene expression can be significant and generally lead to loss of function in Cx32 production. Among the reported mutations, c.–529T>G and c.–527G>C, reside in SOX10 transcription factor binding site and they were shown to cause a reduction in gene expression (Ionasescu *et al*., 1996b; Bondurand *et al*., 2001; Houlden *et al*., 2004). Another mutation (c.–459C>T) was also shown to abolish ribosome entry site of Cx32 mRNA (Ionasescu *et al*., 1996b; Flagiello *et al*., 1998). Lastly, c.–713G>A is an interesting mutation such that it was initially reported as reducing promoter activity after its identification in a Taiwanese family (Wang *et al*., 2000), however, it is considered as a polymorphism in Caucasian population in HGMD (Bergmann *et al*., 2001).

In previous years, three novel variants which are located on non-coding region of *GJB1* gene were identified in our laboratory. Two of these variants (c.-541A>G; c.-528T>C) are located on SOX10 binding site of *GJB1* gene and possibly cause reduced gene expression. Third variant, on the other hand, located at the junction of intron and exon 2 (c.-18A>G). These variants were shown to segregate with the disease phenotype in these families (Erdoğan, 2012). In this study, we aim to investigate the effect of these variants on the expression of *GJB1* gene. In addition, we intend to screen more patients in our Turkish CMT cohort to further identify novel *GJB1* mutations *via* direct sequencing (Table 6.1).

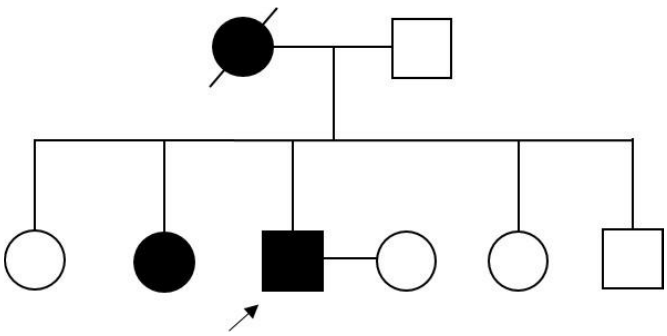

Figure 1.6. Pedigree of family P232.

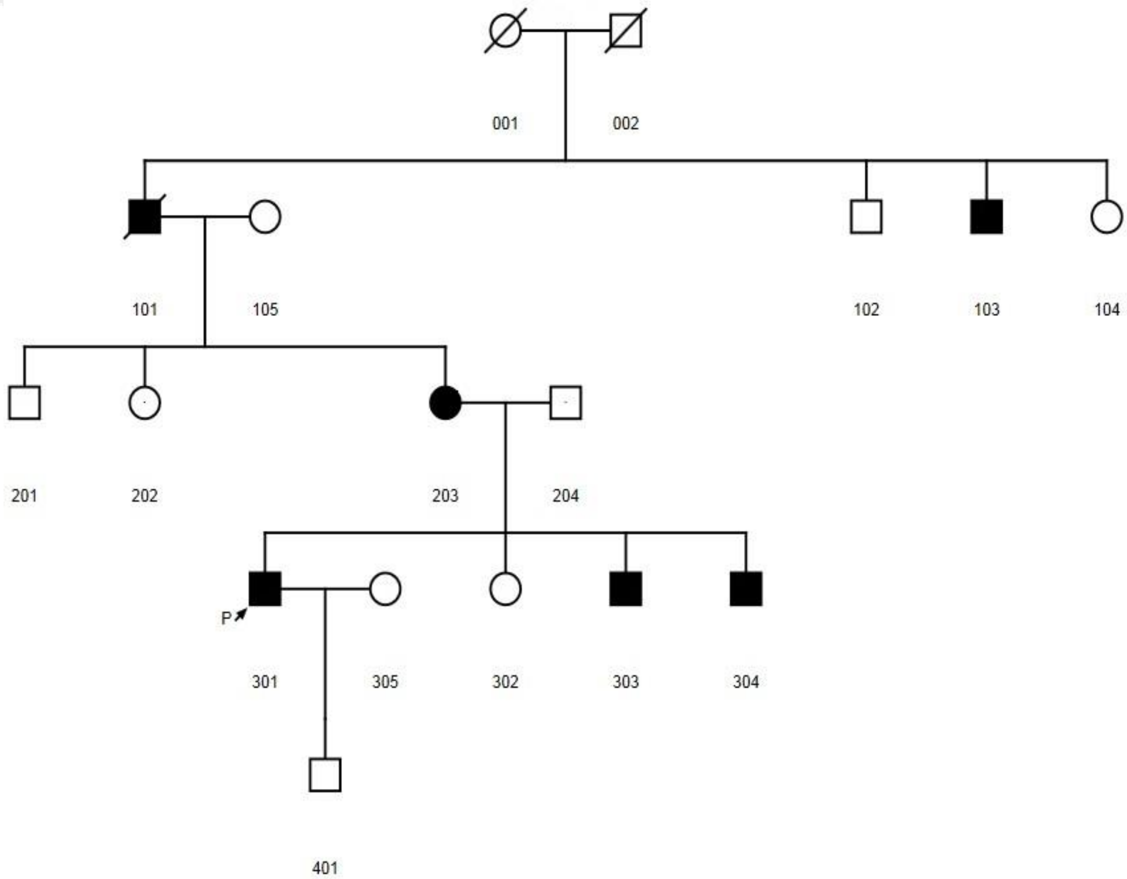

Figure 1.7. Pedigree of family P158.

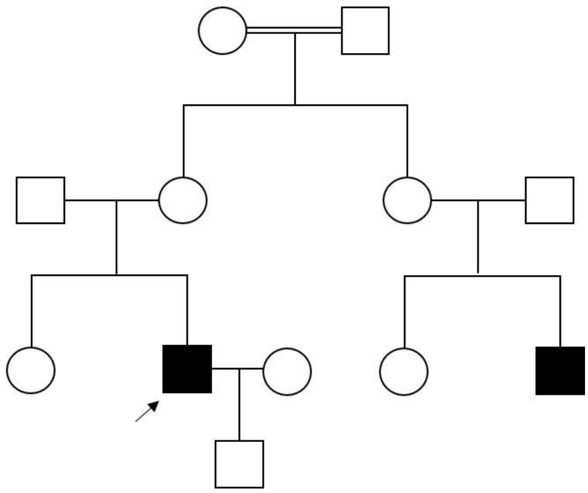

Figure 1.8. Pedigree of family P727.

2. PURPOSE

GJB1 gene mutations are second most common cause of all CMT cases. Causative mutations in both coding and untranslated regions of the gene have increased to 400 in recent years which emphasize the importance of genetic diagnosis. In this study, our first aim was to screen *GJB1* gene of patients with CMT phenotype for novel mutations using PCR-Direct sequencing technique. For this purpose, 50 families that have not been diagnosed for any other CMT gene mutations were analyzed.

We also aimed to investigate the effects of *GJB1* 5'UTR variants that have been identified in our CMT cohort. In few studies in literature, *GJB1* promoter mutations were shown to cause CMT phenotype by reducing the expression of the gene. In this study, we aimed to perform luciferase reporter gene assay in order to determine the effects of specific promoter variants that identified in our laboratory.

3. MATERIALS

3.1. Subjects

Peripheral blood samples of Turkish CMT patients and their family members were provided by various neurology departments around Turkey. Detailed electrophysiological and histopathological features of patients and pedigrees were obtained from clinicians. Informed consent from patients and approval of ethics committee were provided.

3.2. Chemicals

All solid and liquid chemicals used in this study were bought from Merck (Germany), Sigma (USA) and Riedel de-Häen (Germany) unless stated otherwise in the text.

3.3. General Kits, Enzymes, and Reagents

The kits, enzymes, and the reagents used in this study and the companies from which they were purchased are provided in Table 3.1.

Table 3.1. List of kits, enzymes, and reagents.

Dulbecco's Modified Eagle Medium (DMEM)	Gibco, USA
DNA Molecular Weight Marker	GeneRuler 100 bp DNA Ladder, Fermentas, USA
DNA Molecular Weight Marker	GeneRuler 1 kb DNA Ladder, Fermentas, USA
Dual-Glo Luciferase Assay System	Promega, USA
Fetal Bovine Serum (FBS)	Gibco, USA
GeneJET Plasmid Miniprep Kit	Thermo, USA

Table 3.1. List of kits, enzymes, and reagents (cont.)

Gibson Assembly Clonning Kit	NEB, USA
Phusion High-Fidelity DNA Polymerase	Thermo, USA
Phusion Site-Directed Mutagenesis Kit	Thermo, USA
QIAquick PCR Purification Kit	Qiagen, Germany
Restriction Enzymes	NEB, USA
T4 DNA Ligase	Thermo, USA
Taq DNA polymerase	Thermo, USA
Turbofect Transfection Reagent	Thermo, USA
ZymoPURE Maxiprep kit	Zymo,USA

3.4. Biological Materials

3.4.1. Bacterial Strain

DH 5-alpha Competent E. coli bacterial strain (genotype: fhuA2 Δ(argF-lacZ)U169 phoA glnV44 Φ80 Δ(lacZ)M15 gyrA96 recA1 relA1 endA1 thi-1 hsdR17) supplied by Gibson Assembly Cloning Kit (NEB, USA) was used in this study. It is used for transformation and purification of all plasmids.

3.4.2. Mammalian Cell Line

Human embryonic kidney cell line HEK 293T was kindly provided by Prof. Kuyaş Buğra. The cell line was used for transfection experiments.

3.5. Buffers and Solutions

3.5.1. DNA Extraction from Peripheral Blood

The buffers and chemicals used to extract genomic DNA from peripheral blood samples of CMT patients are listed in Table 3.2.

Table 3.2. Buffers and chemicals that were used for DNA extraction from peripheral blood.

Cell Lysis Buffer	155 mM NH4Cl 10 mM KHCO3 1 mM Na_2EDTA (pH 7.4)
Nuclei Lysis Buffer	10 mM Tris-HCl (pH 8.0) 400 mM NaCl 2 mM Na_2EDTA (pH 7.4)
Sodiumdodecylsulphate	10% SDS (w/v) (pH 7.2)
Proteinase K	20 mg/ml
Tris-EDTA (TE) Buffer	20 mM Tris-HCl (pH 8.0) 0.1 mM Na2EDTA (pH 8.0)
5 M NaCl solution	292.2 g NaCl in 1 L dH2O

3.5.2. Polymerase Chain Reaction (PCR)

The list of the buffer and the chemicals used for PCR in this study are provided in Table 3.3.

Table 3.3. The buffer and the chemicals used for PCR.

10 X MgCl2 Free Buffer	100 mM Tris-HCl 500 mM KCl (pH 9.1 at 20°C) (Fermentas, Lithuania)
Magnesium Chloride (MgCl2)	25 mM $MgCl_2$ (Fermentas, Lithuania)

Table 3.3. The buffer and the chemicals used for PCR (cont.).

Deoxyribonucleotide Triphosphates (dNTPs)	100 mM of each dNTP (Fermentas, Lithuania)

3.5.3. Restriction Enzyme Analysis

The restriction enzyme digestions were performed using the buffer given in Table 3.4, to linearize vector for cloning.

Table 3.4. Buffer that used for restriction digestion.

1X CutSmart® Buffer	50 mM Potassium Acetate 20 mM Tris-acetate 10 mM Magnesium Acetate 100 µg/ml BSA pH 7.9 @ 25°C

3.5.4. Agarose Gel Electrophoresis

All PCR, restriction digestion and cloning products were run in agarose gels prepared by ingredients given in Table 3.5.

Table 3.5. Ingredients that are used for Agarose Gel Electrophoresis.

5 X Tris-Borate-EDTA (TBE) Buffer	0.89 M Tris-Base 0.89 M Boric Acid 20 mM Na2EDTA (pH 8.3)
1 or 2% Agarose Gel	1 or 2% Agarose (w/v) (Peqlab, Germany) in 0.5 X TBE Buffer
Ethidium Bromide	10 mg/ml
6 X Loading Buffer	2.5 mg/ml Bromophenol Blue 1% SDS (w/v) in 2 ml glycerol

3.5.5. Bacterial Culture Solutions and Antibiotics

Ingredients and mediums that were used for preparation of bacterial culture were given in Table 3.6.

Table 3.6. Solutions and Antibiotics used for the growth and maintenance of bacterial cultures.

Luria-Bertani medium (LB)	10 g tryptophan 5 g yeast extract 10 g NaCl Distilled water up to 1 L, autoclaved
Luria-Bertani Agar	10 g tryptophan 5 g yeast extract 10 g NaCl 15 g Agar Distilled water up to 1 L, autoclaved
Ampicillin stock	100 mg/ml in 50 % Ethanol Filter-sterilized and stored at -20°C 100 µg/ml (working concentration)
SOC medium	20 g Tryptone 5 g Yeast Extract 2 ml of 5M NaCl 2.5 ml of 1M KCl 10 ml of 1M MgCl2 10 ml of 1M MgSO4 20 ml of 1M Glucose Distilled water up to 1L Filter-sterilized and stored at -20°C

3.5.6. Cell Culture

Mediums and buffers that used for growth and maintenance of HEK293T cells were given in Table 3.7.

Table 3.7. Buffers and solutions used in cell culture.

Complete Medium for HEK293T Cells	DMEM 10% FBS 0.1% Penicillin/Streptomycin 1% Non-essential Amino Acid (PAN-Biotech, Germany)
Freezing Medium for HEK293T Cells	50% DMEM 40% FBS 10% DMSO
1X PBS (Phosphate Buffered Saline)	8 g NaCl 0.2 g KCl 1.44 g Na2HPO4 0.24 g KH2PO4
10X Trypsin-EDTA Solution	2.5% Trypsin 7mM Ethylenediaminetetraacetic Acid (EDTA) 0.9% NaCl diluted with Phosphate Buffered Saline (PBS)

3.6. Nucleic Acids

DNA molecular weight markers and deoxyribonucleotides were purchased from Fermentas (USA).

3.6.1. Plasmids

pGL2-basic Luciferase vector (Promega, USA) was commercially obtained. SOX10 expression vector was commercially obtained from Origene, USA. pRL-SV40 (Renilla Luciferase) plasmid was kindly provided by Dr. Necla Birgül İyison.

3.6.2. Oligonucleotides

Primers used in polymerase chain reactions, sequencing, cloning and site-directed mutagenesis were purchased from Macrogen Inc. (Seoul, South Korea) and are listed accordingly in Tables 3.8 - 3.12.

Table 3.8. Sequence of the primers used for exon amplification of *GJB1* for PCR and Sanger sequencing.

Region	**Primer (F/R)***	**Primer sequence (5'-3')**	**Annealing Temp. (°C)**	**Product size (bp)**
Exon 1	Cx32-1F	TGAGGCAGGATGAACTGGACAGGT	59	306
	Cx32-1R	TTGCTGGTGAGCCACGTGCATGGC		
	Cx32-2F	ATCTCCCATGTGCGGCTGTGGTCC	63	432
	Cx32-2R	GATGATGAGGTACACCACCT		
	Cx32-3F	CGTCTTCATGCTAGCTGCCTCTGG	60	304
	Cx32-3R	TGGCAGGTTGCCTGGTATGT		

Table 3.9. Sequence of the primers used for 5'UTR amplification of *GJB1* for PCR and Sanger sequencing.

Region	**Primer (F/R)***	**Primer sequence (5'-3')**	**Annealing Temp. (°C)**	**Product size (bp)**
5' UTR	5'UTR-GJB1-F	CTCAGGGAAAATCCTGGTGA	67.5	989
	5'UTR-GJB1-R	TCATCACCCCACACACTCTC		

Table 3.10. Sequence of the primers used to linearize pGL2-GJB1 plasmid to generate c.-541A>G variant by site-directed mutagenesis.

Region	**Primer (F/R)***	**Primer sequence (5'-3')**	**Annealing Temp. (°C)**	**Product size (bp)**
pGL2-GJB1	pGL2-541-F	GTTGTTCAGAGCCCCGCAAAGGTCTCATTG	72	6587
	pGL2-541-R	GCCCTTTAGAATTCAGATCAAACGCCCTGAC		

Table 3.11. Sequence of the primers used for colony PCR.

Region	**Primer (F/R)***	**Primer sequence (5'-3')**	**Annealing Temp. (°C)**	**Product size (bp)**
pGL2	GL-F	TGTATCTTATGGTACTGTAACTG	55	1090
	GL-R	CTTTATGTTTTTGGCGTCTTCCA		

Table 3.12. Sequence of the primers used to amplify insert DNA for Gibson Assembly.

Region	**Primer (F/R)***	**Primer sequence (5'-3')**	**Annealing Temp. (°C)**	**Product size (bp)**
5'UTR	GJB1-insert-F	CTGTAACTGAGCTAACATAACCCCTCAGGGAAAATCCTGGTG	72	1028
	GJB1-insert-R	CGTAAGAGCTCGGTACCTCCCTCATCACCCCACACACTC		

3.7. Disposable Labware

Table 3.13. List of disposable labware used in this study.

Centrifuge Tubes (15 ml, 50 ml)	TPP, Switzerland
Microfuge Tubes (1.5 ml, 2 ml)	Axygen, USA
PCR Tubes (0.2 ml)	Axygen, USA
Cell Culture Plates (10 cm, 6-well, 96-well)	TPP, Switzerland
Cell Scraper	TPP, Switzerland
Serological Pipettes (5 ml, 10 ml, 25 ml)	Capp, Denmark
Pipette Tips (Filtered)	Capp, Denmark
Pipette Tips (Bulk)	Axygen, USA
96-well plates for Luciferase Assay	Roche, Switzerland

3.8. General Equipment

The equipment used in this study are listed in Table 3.14.

Table 3.14. Equipment used during this study.

Autoclave	Model MAC-601 (Eyela, Japan)
Centrifuges	Centrifuge 5415C (Eppendorf, Germany) Allegra X-22R Centrifuge (Beckman Coulter, USA)
Deep Freezers	-20°C (Bosch, Germany) -20°C (Arçelik, Turkey) -70°C (Thermo Forma, USA)
Documentation System	GelDoc Documentation System (Bio-Rad, USA)
Electrophoresis Equipments	Mini-Sub Cell (Bio-Rad, USA) PROTEAN Vertical Electrophoresis System (Bio-Rad, USA)

Table 3.14. Equipment used during this study (cont.).

Incubators	DRI Block DB-2A (Techne, UK) Shake'n'Stack (Hybaid, UK) Oven EN400 (Nuve, Turkey)
Luminometer	Fluoroskan Ascent FL, Thermo Electron, USA
Magnetic Stirrer	Speed Safe (Hanna Instruments, USA) MK 418 (Nüve, Turkey)
Oven	Microwave Oven (Vestel, Turkey)
Power Supplies	Power Pac Model 3000 (Bio-Rad, USA) PS 304 (Apelex, France)
Refrigerator	+4°C (Arçelik, Turkey)
Shaker	SL 350 (Nüve, Turkey)
Spectrophotometer	NanoDrop ND-1000 (NanoDrop, USA)
Thermal Cyclers	Icycler (Bio-Rad, USA) Mycycler (Bio-Rad, USA) Runik Thermal Cycler (Sacem, Turkey) C 1000 Thermal Cycler (Bio-Rad, USA)
Vortex	Nuvemix (Nuve, Turkey)

4. METHODS

4.1. DNA Extraction from Peripheral Blood

Ten ml of blood sample were collected in K_3EDTA tubes from each patient and their available family members. Before DNA extraction, the samples were stored at 4˚C. Blood samples were transferred into sterile 50 mL centrifuge tubes. First, 30 mL red blood cell (RBC) lysis buffer was added to 10 mL of blood sample in order to lyse the erythrocyte membranes and left at 4˚C for 25 minutes. The lysed samples were centrifuged at 5000 rpm, at 4˚C for 10 min. After discarding the supernatant, 10 mL RBC lysis buffer was added to the samples. The pellet was resuspended completely by vortex and centrifugation was repeated at 5000 rpm, at 4 ˚C for 10 minutes. The supernatant was discarded and 5 mL nuclei lysis buffer, 40 µl Proteinase K and 50 µl of 10% SDS were added to the pellet. Thereafter, the samples were incubated at 37˚C overnight in order to degrade cellular proteins. The next day, 10 mL of 2.5 M NaCl were added, the samples were vortexed and centrifuged at room temperature at 5000 rpm for 30 minutes. The supernatant was transferred into a new 50 mL centrifuge tube. After addition of 2 volume of absolute ethanol (-20˚C), the DNA was precipitated. The genomic DNA was taken into a 1.5 mL microcentrifuge tube and allowed to air-dry. Accordingly the DNA was dissolved in 100-300 µl of Tris-EDTA (TE) buffer and stored at -20˚C.

4.2. Quantitative Analysis of Purified DNA

Nanodrop ND-1000 spectrophotometer was used to measure the genomic DNA concentration at 260nm. The main principle of the measurement was based on the fact that absorbance of 50 µg of pure double stranded DNA has an absorbance of 1.0 at 260 nm. To ensure the purity of DNA A260/A280 ratio should be around 1.8. Moreover, A260/A230 ratio should be higher than 2.0 to implicate low salt concentration.

4.3. Mutation Analysis

In this study, 50 Turkish CMT patients were screened for mutations in *GJB*1 gene. The patients were selected from our cohort based on their pedigree pattern for X-linked inheritance and presence of intermediate (30-45m/sec) motor median nerve conduction velocity (MM-NCV). They were previously found to be negative for CMT1A duplication and HNPP deletion. All selected patients were screened for 5'UTR of *GJB1* gene and 36 of them were screened for both coding sequence (CDS) and 5'UTR of *GJB1* gene.

4.3.1. Mutational Analysis of CDS and 5' UTR of *GJB1* by PCR-Direct Sequencing

Direct sequencing was an efficient and fast method to detect variants in the PCR amplified DNA sequences. PCR was repeated when non-specific or weak bands were obtained on the agarose gels either by changing the cycle conditions or concentrations of the chemicals. PCR was performed in a total volume of 50 μl with chemical concentrations described in Table 4.1.

Table 4.1. PCR for CDS and 5'UTR amplification of *GJB1*.

Ingredient	**Volume (μl)**
DNA (50ng)	4
Taq DNA polymerase buffer (10X)	5
$MgCl_2$ (25mM)	5
dNTPs (0.1 mM)	1
Forward and Reverse Primers (10pmol/μl)	2 from each
Taq DNA Polymerase (1 Unit)	0.2
dH_2O	30.8

Conditions used in PCR are given in Table 4.2. Sequence of primers that were used in PCR and their annealing temperatures were depicted in Table 3.7-3.8. In order to check the size of amplicons and to ensure absence of non-specific bands, a mixture of 5 µl of PCR product and 1 µl of agarose loading buffer was loaded on 2% (w/v) agarose gel. 100 bp DNA size marker (SM0241, Fermentas, USA) was used to confirm the size of the amplicon.

Table 4.2. Conditions of PCR for CDS and 5'UTR of *GJB1*.

Conditions of PCR	
Initial denaturation	5 min at 95ºC
Denaturation (35 cycles)	30 s at 95ºC
Annealing (35 cycles)	30 s at annealing temperature
Extension (35 cycles)	45 s at 72ºC
Final Extension	3 min at 72ºC
Cooling	1 min at 4ºC

Sequencing of amplified DNA products were commercially performed by Macrogen Inc, Korea. Results were analyzed by Ape software.

4.4. Molecular Cloning

4.4.1. PCR Amplification of Insert DNA

DNA sequence of 5'UTR of *GJB1* were amplified using the Phusion High-Fidelity DNA Polymerase (Thermo, USA) for cloning. Genomic DNA of patients that carry specific variants to be tested (c.-18A>G, c.-528T>C and c.-713G>A) and of one healthy individual were used as DNA templates for amplication. Template DNA concentration was, 200 ng in the amplification reaction mixture. PCR reactions were carried out according to manufacturer's instructions by using primers shown in Table 3.11. These primers contain at least 20 bp overhangs that are complementary to vector ends in order to accomplish cloning by Gibson Assembly reaction. The protocol for Phusion polymerase is summarized in Table 4.3.

Table 4.3. PCR protocol using the Phusion High-Fidelity DNA Polymerase.

Step #	Description	Temperature (°C)	Duration
1	Initial denaturation	98	30 s
2	Denaturation	98	10 s
3	Annealing	Primer specific Tm	10s
4	Elongation	72	15 s per 1 kb
5	Return to Step 2 (x30)	-	
6	Final Elongation	72	5 min

Table 4.4. Ingredients for PCR using the Phusion High-Fidelity DNA Polymerase.

Ingredient	Volume (µl)
Template DNA	varies
5X Phusion HF Buffer	10
dNTPs (10 mM)	1
Forward and Reverse Primers (10pmol/µl)	2 from each
Phusion DNA Polymerase (2 Unit)	0.5
dH_2O	Add to 50 µl

4.4.2. Restriction Digestion of Vector

Restriction digestion of pGL2-basic vector was carried out with SmaI restriction enzyme (NEB, USA) at 37 ºC for 1 hour in 1X CutSmart buffer (Table 3.4). One unit of enzyme was used for digestion of 1µg of DNA. Heat inactivation of the restriction enzyme was performed at 65ºC for 20 min.

4.4.3. Agarose Gel Electrophoresis

PCR products and linearized vector were run by electrophoresis using standard 1 or 2% Agarose (w/v) in 0.5 X TBE Buffer. Agarose powder was mixed with 0.5X TBE Buffer and allowed to boil in a microwave oven. After cooling for a couple of minutes, ethidium bromide was added to a final concentration of 10 mg/ml and the solution was poured into the gel casting tray. Appropriate amounts of the DNA samples were mixed with 6X loading buffer to get 1X final concentration. Gene Ruler 100 bp and/or 1kb DNA ladder (Fermentas, USA) were used as molecular weight markers. The solidified gels were run in 0.5X TBE buffer at varying voltage and time depending on the size the fragments. The gels were visualized under UV light and the images were documented with GelDoc imaging system (BioRad, USA).

4.4.4. PCR Purification

PCR products were purified with spin columns using the PCR purification kit (Qiagen, Germany) according to manufacturer's instructions.

4.4.5. Gibson Assembly Cloning

Amplified 5'UTR of *GJB1* fragments were cloned in pGL2-basic vector using the Gibson Assembly kit (NEB, USA). In brief, the Gibson assembly reaction contains three enzymes; a 5'-exonuclease that removes nucleotides from the 5'-ends of DNA fragments, effectively creating 3' overhangs, a DNA polymerase that fills in the gaps of annealed DNA fragments, and a DNA ligase that seals the nicks between the fragments. DNA fragments to be ligated were prepared with at least 20bp overhangs by PCR amplification as described in section 4.4.1. Vector backbones were digested by SmaI restriction enzyme (NEB, USA) in order to produce a linear vector as described in Section 4.4.2. All fragments to be used in the subsequent assembly reaction were purified by QIAquick PCR Purification kit (Qiagen, Germany) prior to the assembly (Section 4.4.4). The suggested molarities of DNA fragments for optimal yield were between 0.02 - 0.1 pM. Molarities were calculated using a dedicated online tool from the NEB website (http://nebiocalculator.neb.com) and DNA concentrations were measured using NanoDrop Spectrophotometer. The molarities were 0.01 pM for insert fragments and 0.03 pM for the vector backbone. The reaction mixture was prepared according to Table 4.5 and was incubated at 50 ºC for 1 hour. Thereafter, 1-5 µl of the assembly reaction were transformed to chemically competent bacteria provided with the kit.

Table 4.5. Ingredients for Gibson Assembly reaction.

Amount of DNA Fragments	0.02–0.5 pmoles
Gibson Assembly Master Mix (2X)	10 µl
Deionized H_2O	Add to 20 µl
Total Volume	20 µl

4.4.6. Transformation of Competent Cells

A vial (50-100 µl) of competent cells was thawed on ice for 10-15 min. 1-5 µl of assembly reaction was added onto the competent cells and incubated on ice for 15-20 min. The vial was placed in 42ºC heat block for 30 seconds to allow heat shock and then transferred immediately on ice for 2 min. SOC medium at room temperature (950 µl) was added and the cells were incubated at 37ºC for 1 hour with shaking at 250 rpm. At the same time, LB-agar plates were warmed at 37ºC. Then, 50-100 µl of mixture was spread onto ampicillin containing LB plates and incubated overnight at 37ºC in inverted position.

4.4.7. Colony PCR

Colony PCR reaction was prepared in a total volume of 25 µl as follows: 1X Taq Polymerase Buffer, 2 mM $MgCl_2$, 0.25 mM dNTP mixture, 5 per cent DMSO, 0.4 µM of each primer, and 0.05u/µl Taq DNA polymerase (Thermo). As the template for PCR, 5-10 bacterial colonies from each of the transformation plates were picked up using autoclaved tips and transferred to the corresponding PCR tubes. The conditions of PCR is given in Table 4.6.

Table 4.6. Conditions of Colony PCR.

Conditions of Colony PCR		
Initial denaturation		5 min at 95ºC
Denaturation	35 cycles	30 s at 95ºC
Annealing	35 cycles	30 s at 55ºC
Extension	35 cycles	1 min at 72ºC

Table 4.6. Conditions of Colony PCR (cont.).

Final Extension	5 min at 72ºC
Cooling	1 min at 4ºC

4.4.8. Plasmid DNA Purification and Sequencing

Plasmid DNA purification were performed from overnight grown bacterial cultures using GeneJET Miniprep Kit and ZymoPURE Maxiprep Kit according to the manufacturer's protocol. Products of minipreps were further purified by phenol:chloroform and ethanol precipitation in order to remove endotoxins. Quality and concentration of the isolated plasmids were determined by spectrophotometric measurements using a NanoDrop-1000 spectrophotometer. Plasmid preparations with OD260/280 ratios between 1.8 and 2.0 were further used for sequencing. Sanger sequencing was performed by Macrogen Inc. (South Korea) using sequencing primers. The bacterial cells carrying the plasmids with the desired fragments were stocked by adding 10% glycerol into overnight bacterial culture and stored at -80ºC until used.

4.4.9. Phenol-Chloroform and Ethanol Precipitation

A mixture of 100 µl DNA and 300 µl of TE buffer was prepared. An equal volume (400 µl) of phenol-chloroform solution was added. Mixture was centrifuged at 5000rpm for 5 min at RT. Upper phase was removed into a fresh tube and TE buffer was added to complete the volume to 400 µl again. Na-Ac (3M) of 40 µl was added and vortexed. After addition of 1mL absolute ethanol, mixture was left at -80 ºC for 30 min or -20 ºC for overnight. Then, the mixture was centrifuged at 4 ºC for 20 min at 5000 rpm. Supernatant was discarded and pellet was washed with 200 µl of 70% cold (-20 ºC) ethanol by spinning at 5000 rpm for 10 min at 4 ºC. Wash step was repeated and pellet left to dry before re-suspended in 50 µl TE buffer.

4.5. Site-Directed Mutagenesis

The variant of c.-541A>G has been identified in family P232 in our CMT cohort however genomic DNA of affected individuals were not available. Therefore, it was not possible to amplify the DNA fragment containing c.-541A>G variant from the affected individuals. Instead, this variant was generated on the plasmid containing wild type sequence of 5'UTR of *GJB1* gene via site-directed mutagenesis.

4.5.1. Linearization of Plasmid by PCR

pGL2-GJB1 plasmid that contains the wild type 5'UTR *GJB1* fragment was linearized by PCR with Phusion High-Fidelity *Taq* polymerase. As template DNA, 20 ng of pGL2-GJB1 plasmid was used. Primers that contain c.-541A>G variant was used in the PCR. The conditions and ingredients of the reaction were given in Tables 4.2 and Table 4.3, respectively.

4.5.2. Non-Radioactive Phosphorylation with T4 PNK

The linearized plasmid was phosphorylated at its 5'end before ligation reaction. For this purpose, a reaction mixture was prepared on ice as given in Table 4.7.

Table 4.7. Ingredients for phosphorylation by T4 PNK.

DNA	up to 300 pmol
T4 PNK Reaction Buffer (10X)	5 µl
ATP (10 mM)	5 µl
T4 PNK	1 µl (10 units)
dH_2O	Add to 50 µl

4.5.3. Ligation of Plasmid

The phosphorylated PCR product was circularized using T4 DNA Ligase in a 5 minutes reaction at 25 ºC. The reaction mixture given in Table 4.8 was prepared on ice and briefly vortexed before incubated at room temperature (25 ºC) for 5 min.

Table 4.8. Ingredients for ligation reaction by T4 DNA Ligase.

DNA	10-20 ng
5X Rapid Ligation Buffer	2 µl
T4 DNA Ligase	0.5 µl
dH_2O	Add to 9.5 µl

After incubation, 1-5 µl of circularized product was used to transform competent bacteria and purify plasmid DNA according to instructions on sections 4.4.6-4.4.9.

4.6. Cell Culture Experiments

4.6.1. Maintenance of HEK293T Cells

HEK293T cells were maintained in their complete medium (Table 3.7) in an incubator at 37ºC, with 5% CO_2. When the plates reached 90% confluence, the cells were washed with PBS, treated with 0.25% trypsin-EDTA solution (Table 3.7) for 5 minutes at 37^0C and then equal volume of complete medium was added prior to scraping. The scraped cells were pelleted by centrifugation at 500 g for 5 minutes and, after resuspension in 3 mL complete medium, they were divided into three plates. On each plate, 7 mL of fresh complete medium was added and plates were incubated in the same conditions. Media were kept at 4ºC and warmed to 37ºC in a water bath before each use.

4.6.2. Freezing of HEK293T Cells

Mammalian cells can be frozen as stocks until further usage. Plates with ~90% confluency can be stocked in freezing medium (Table 3.7). The medium over the cells was aspirated and the cells were washed with 1X PBS. Then, trypsin was added onto the cells and incubated at 37ºC for 5 minutes. Equal volume of fresh medium was added and cells were harvested by scrapping. The cell suspension was transferred into a 15 ml Falcon tube and precipitated by centrifugation at 500 g for 5 minutes. Cell pellet was resuspended in 1 ml of freezing medium and stored at -80ºC.

4.6.3. Thawing of HEK293T Cells

The frozen cell stocks were thawed in a water bath at 37 °C and centrifuged at 500 g for 5 min in order to remove DMSO. Then, the cell pellet was resuspended in 1 ml of fresh complete medium and transferred to 10 cm culture dishes containing 7 ml of complete medium.

4.6.4. Transfection of HEK293T Cells

Transfections were performed by using the Turbofect transfection reagent (Thermo Scientific Inc., USA) according to the manufacturer's instructions. One day before transfection, 100.000 cells were seeded on 12-well plate and left to grow in incubator at 37ºC, with 5% CO_2 for 24 hours. Next day, transfection complex was formed in pure DMEM-only without any FBS or antibiotics and added drop by drop over the attached cells on plate after incubation at room temperature for 15 minutes. Approximately 4 hours after transfection, medium was replaced with fresh complete medium.

Seven different plasmids were used for transfections: Five of them were pGL2 luciferase vectors that contain 5'UTR of *GJB1* gene, a SOX10 transcription factor expression plasmid in order to activate *GJB1* gene expression, and pGL3-SV40-Renilla, as internal control plasmid.

5'UTR of *GJB1* gene contains two SOX10 binding sites. Expression of the gene is initiated by binding of SOX10 protein to these sites. Therefore, SOX10 expression vector was transfected into HEK293T cells along with luciferase vector constructs containing 5’UTR sequence of *GJB1* gene. Plasmids that are used in transfection experiment are listed in Table 4.9.

Table 4.9. Plasmids used in transfection experiments.

Plasmid	Variant	Amount (ng/well)
pRL-SV40	-	50
pGL2-GJB1	c.-18A>G	500
pGL2-GJB1	c.-541A>G	500
pGL2-GJB1	c.-528T>C	500
pGL2-GJB1	c.-713G>A	500
pGL2-GJB1	-	500
SOX10	-	1500

4.7. Luciferase Reporter Assay

Luciferase assay was performed according to Dual-Glo Luciferase Assay System (Promega) protocol to determine any change in promoter activity due to *GJB1* promoter variants. For the assay, cells were co-transfected with 500 ng of a pGL2-luciferase reporter plasmid including 5’UTR of *GJB1* gene with or without desired variants, 50 ng of pRL-SV40-Renilla (internal control), and 1.5 µg of SOX10 expression plasmid per well of a 12-well plate. About 48 hours post-transfection, cells were collected by trypsin, and then washed with 1X PBS twice. Pellet was completely resuspended in 100 µl 1X PBS and placed into 96-well plate. Then, 100 µl of Firefly luciferase substrate reagent added on to the lysates, and after 30 min incubation at room temperature (in the dark), measurements were taken 3 times using a fluorometer (Fluoroskan Ascent FL, Thermo Electron). Next, 100 µl of Renilla luciferase substrate reagent (Stop&Glo) that also quenches the Firefly luciferase luminescence was added and after 10 min incubation at room temperature (in the dark), measurements were taken 3 times. Luminescence reads were taken at 2 seconds of integration time. Firefly luciferase readings were normalized to Renilla luciferase readings and graphs were plotted in Microsoft Excel. T-test was used to evaluate statistically significant differences between the values in Microsoft Excel. All experiments were performed in duplicates and independently validated with three replicates.

5. RESULTS

In the first part of this study, 50 CMT patients in our cohort were selected according to their clinical and electrophysiological features in order to identify *GJB1* gene mutations. These patients were previously found to be negative for CMT1A duplication and HNPP deletion. All patients were analyzed for 5'UTR of *GJB1* gene *via* direct sequencing. Thirty six of these 50 patients were also screened for mutations in the coding region of *GJB1* gene.

In the second part of the study, the effect of four *GJB1*-5'UTR variants on gene expression was investigated by luciferase reporter gene assay.

5.1. Mutational Analysis

Patients were selected according to their electrophysiological and clinical features in addition to pedigree analysis. CMTX1 belongs to intermediate sub-type of CMT and affected individuals generally show NCV values between 25-45 m/s. In pedigree analysis, X-linked segregation of CMT phenotype was considered since *GJB1* gene is located on X-chromosome. Genomic DNA samples of fifty patients were screened for mutations in the only exon and 5'UTR of *GJB1 via* direct sequencing. After amplification of related sequences by PCR and cleaning, sequencing were performed by Macrogen Inc., Korea. Sequence data were analyzed in Ape software. For all samples, NC_000023.11 sequence and ENST00000374022.3 transcript were used as references.

5.1.1. Mutational Analysis of *GJB1* coding sequence

Mutation screening revealed five different *GJB1* variants in eight among 36 patients. Frequencies of all variants were not available in ExAC database due to very rare occurrence.

First variant was identified in two members of a family. The mother (P1020) was found to be heterozygous while her son (P1021) was hemizygous for the c.379A>C variant. Moreover, the same variant was also identified in another hemizygous male patient (P1186) from a different family (Figure 5.1). This variant was not found in dbSNP, IPN Mutation and HGMD databases. However, c.379A>T transition from the same position was previously reported by Qiao *et al*., in 2009. The c.379A>T mutation causes I127F change in amino acid level and shown to be pathogenic (Vondracek *et al*. 2005).

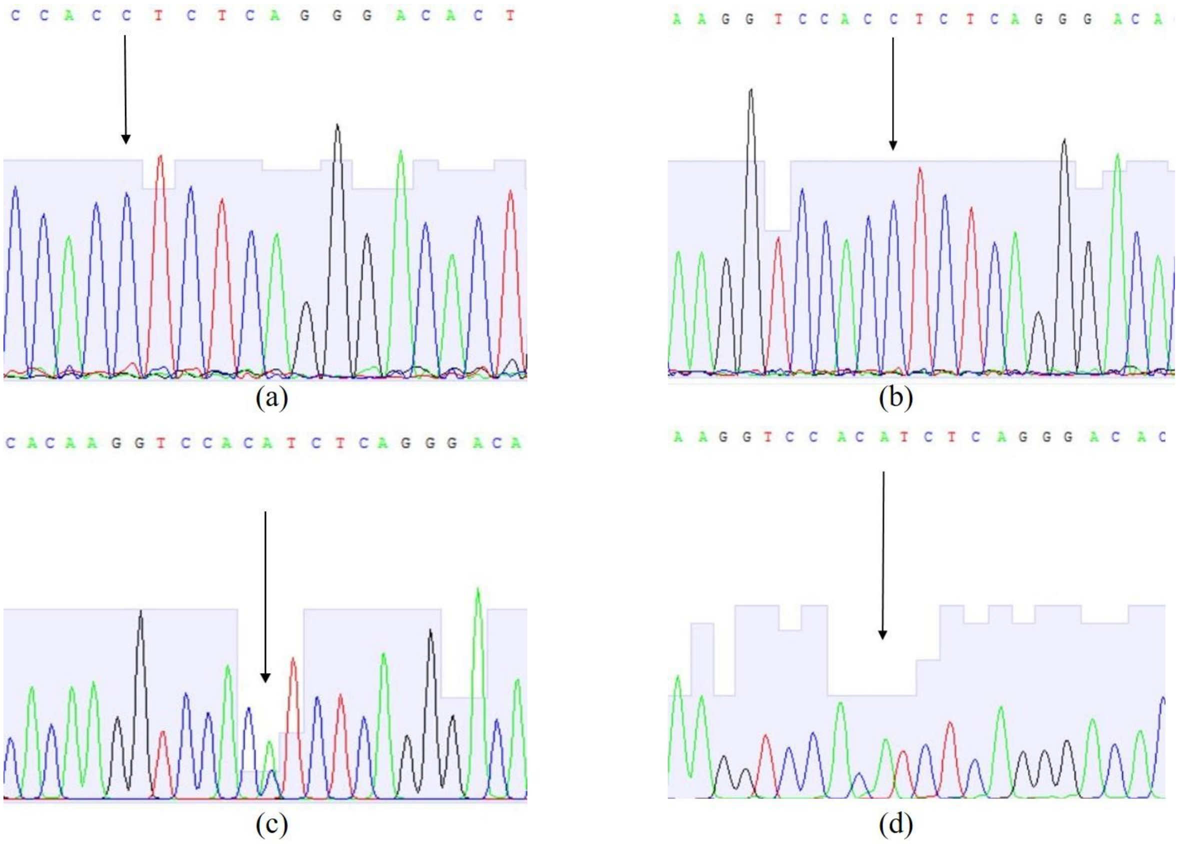

Figure 5.1. (a), (b) Chromatograms showing hemizygous c.379A>C for male patients (P1021 and 1186, respectively) (c) heterozygous female patient (P1020) and (d) the sequence for the male control.

The c.379A>C variant causes Isoleucine to Leucine transition at 127th amino acid position. Although these two amino acids have similar molecular structure, Isoleucine is highly conserved at that position among mammalian species (Figure 5.2) implicating a novel mutation.

Homo sapiens	VKRHKVH $\boxed{\mathbf{I}}$ SGTLWWT
Pan troglodytes	VKRHKVH $\boxed{\mathbf{I}}$ SGTLWWT
Macaca mulatta	VKRHKVH $\boxed{\mathbf{I}}$ SGTLWWT
Canis lupus	VKRHKVH $\boxed{\mathbf{I}}$ SGTLWWT
Bos taurus	VKRHKVH $\boxed{\mathbf{I}}$ SGTLWWT
Mus musculus	VKRHKVH $\boxed{\mathbf{I}}$ SGTLWWT
Rattus norvegicus	VKRHKVH $\boxed{\mathbf{I}}$ SGTLWWT

Figure 5.2. Conservation of Isoleucine at 127th amino acid position among mammalian species, marked by black box.

Second variant of *GJB1* was found in one male and one female patient from different families. The male patient (P1113) was found to be hemizygous for the c.43C>T variant. The affected female (P553), on the other hand, was heterozygous for the same variant, as expected (Figure 5.3).

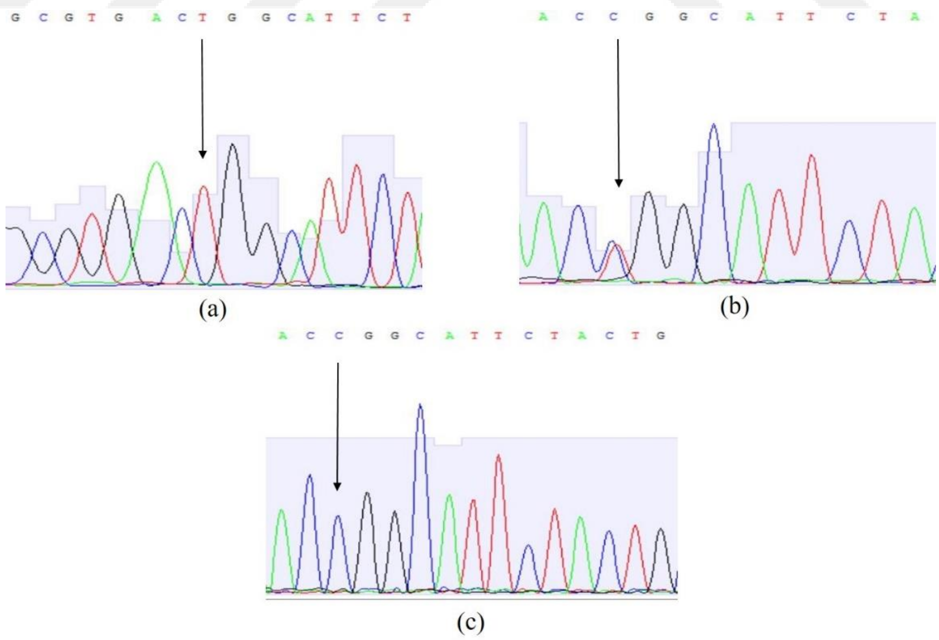

Figure 5.3. (a) Chromatograms showing hemizygous c.43C>T change for male patient (P1113) (b) heterozygous c.43C>T change for female patient (P553) and (c) male control.

The c.43C>T mutation causes R15W change in amino acid level and it was previously reported by Janssen *et al*. in 1997.

The third variant was c.622G>A transition observed in a male patient (P763) (Figure 5.4). This mutation leads to E208K change in amino acid level and previously reported by Fairweather *et al*. in 1994.

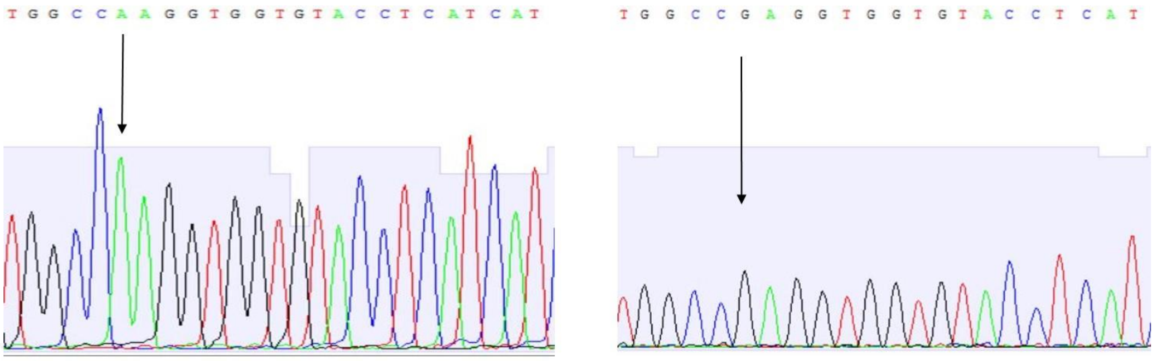

(a) (b)

Figure 5.4. (a) Chromatograms showing hemizygous c.622G>A change for male patient (P763) and (b) male control.

The fourth variant in coding region of *GJB1* gene was identified in a male patient (P1027-3). The patient was hemizygous for c.502T>A variant (Figure 5.5). This variant was not found in dbSNP, IPN Mutation and HGMD databases, instead, c.502T>C transition from the same position was previously reported by Choi *et al*., in 2004 and causes pathogenic C168R transition. On the other hand, c.502T>A variant causes Cysteine to Serine transition at 168th amino acid position. Since Cysteine is highly conserved at that position among mammalian species (Figure 5.6), this variant can be designated as novel mutation.

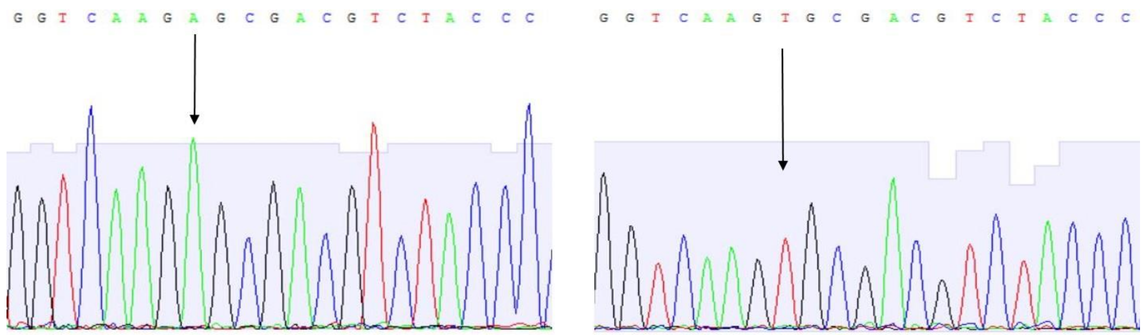

(a) (b)

Figure 5.5. (a) Chromatograms showing hemizygous c.502T>A change for male patient (P1027-3) and (b) male control.

Homo sapiens	AMVRLVK	**C**	DVYPCPN
Pan troglodytes	AMVRLVK	**C**	DVYPCPN
Macaca mulatta	AMVRLVK	**C**	DVYPCPN
Canis lupus	AMVRLVK	**C**	EAYPCPN
Bos taurus	AMVRLVK	**C**	DAYPCPN
Mus musculus	AMVRLVK	**C**	EAFPCPN
Rattus norvegicus	AMVRLVK	**C**	EAFPCPN

Figure 5.6. Conservation of Cysteine at 168th amino acid position among mammalian species, marked by black box.

The fifth and the last variant in *GJB1* coding sequence was observed in a female patient (P711) that was found to be heterozygous for c.47A>T (Figure 5.7). The mutation causes H16L change in amino acid sequence and it was previously published by Keckarevic-Markovic in 2009.

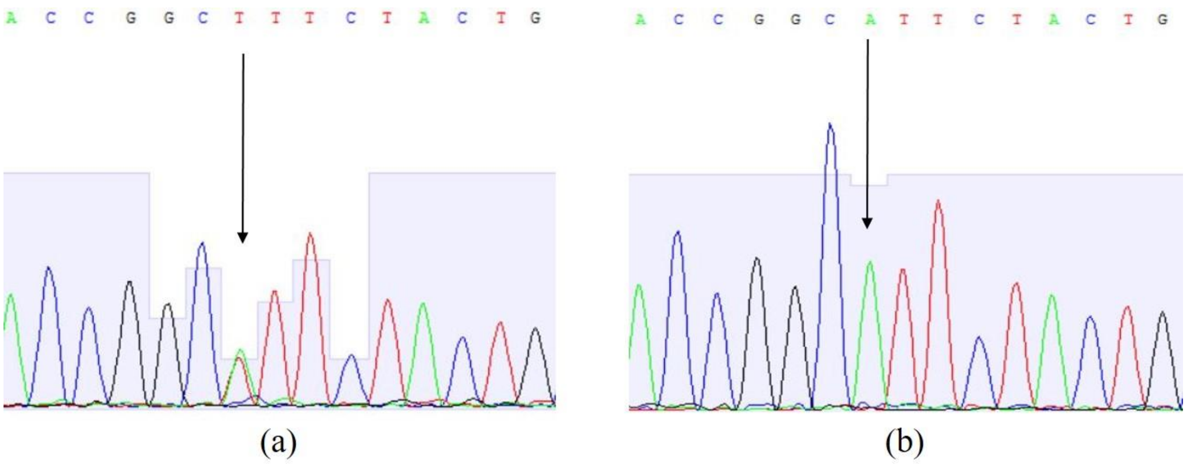

Figure 5.7. (a) Chromatograms showing heterozygous c.47A>T change for female patient (P711) and (b) male control.

5.1.2. Mutational Analysis of 5'UTR of *GJB1*

GJB1 5'UTR was also screened for mutations using PCR and subsequent direct sequencing techniques. Among 50 patients analyzed, three different variants were observed in 25 different patients. All of those 25 patients were found to have c.-713G>A variant. This variant was initially reported as a promoter site mutation by Wang *et al*., 2000, however, it was considered as a Caucasian population polymorphism in dbSNP, 1000 Genome and HapMap databases with a minor allele frequency (MAF) of 0.29.

Second variant in the 5'UTR of *GJB1* was identified in two male patients, P980 and P1256. This variant (c.-18A>G) has been previously observed in family P158 in our laboratory (Erdoğan, 2012). It corresponds to the second last base of the intron 1 of *GJB1* and was predicted as removing the splice site by Human Splicing Finder software (http://www.umd.be/HSF/).

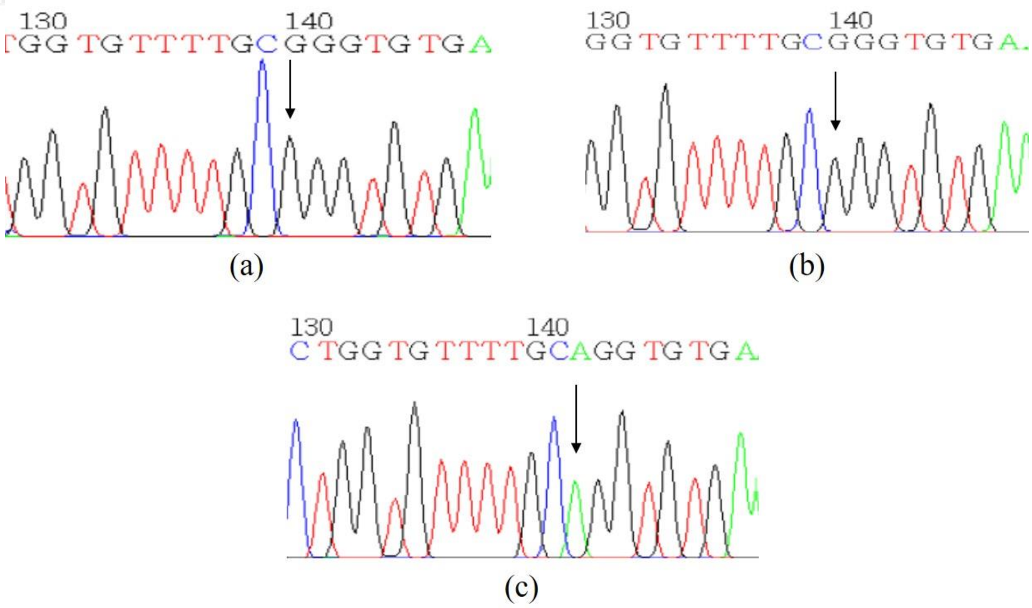

Figure 5.8. (a), (b) Chromatograms showing hemizygous c.-18A>G change for male patients (P980 and P1256, respectively) (c) male control.

The last variant in the 5'UTR of *GJB1* was c.-257C>T change that was observed in a female patient, P374. This intronic variant was considered as a polymorphism in dbSNP, 1000 Genome, and HapMap databases.

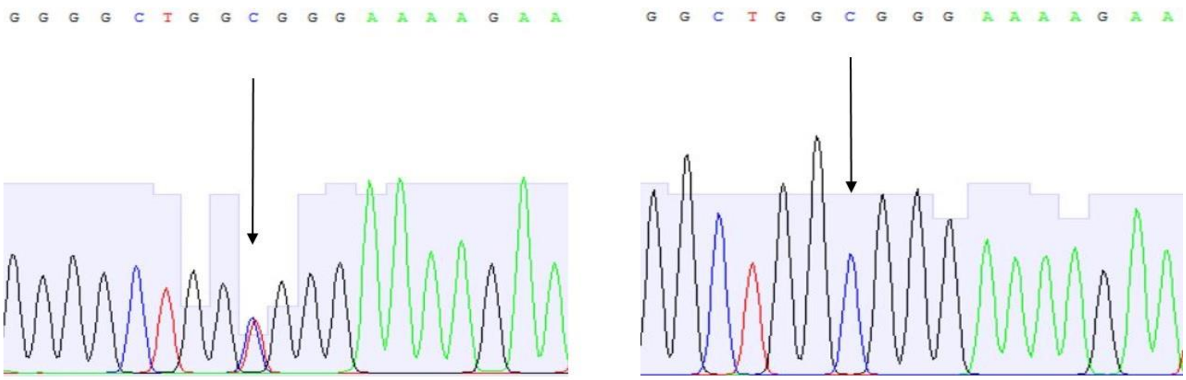

(a) (b)

Figure 5.9 (a) Chromatograms showing heterozygous c.-257C>T change for female patient (P374) (b) male control.

The mutations identified in this study and clinical presentation of the patients with these mutations are summarized in Table 5.1.

Table 5.1. The mutations and the clinical data of the patients.

Patient ID	Gender	Variant	Amino Acid Change	MM-NCV (m/s)	Age of Onset (years)	HGMD #
P1021	M	c.379A>C	p.Ile127Leu	44	2-10	-
P1020	F	c.379A>C	p.Ile127Leu	N/A	N/A	-
P553	F	c.43C>T	p.Arg15Trp	34.5	11-20	CM970654
P1113	M	c.43C>T	p.Arg15Trp	31	11-20	CM970654
P763	M	c.622G>A	p.Glu208Lys	30	21-40	CM940837
P1027-3	M	c.502T>A	p.Cys168Ser	41	11-20	-
P711	F	c.47A>T	p.His16Leu	N/A	N/A	CM095432
P727	M	c.-528T>C	-	37	11-20	-
P232	M	c.-541A>G	-	33.3	11-20	-

Table 5.1. The mutations and the clinical data of the patients (cont.)

P1183	M	c.-713G>A	-	46.5	35	CR001858
P871	M	c.-713G>A	-	24.5	26	CR001858
P158	M	c.-18A>G	-	31	2-10	-
P980	M	c.-18A>G	-	37	28	-

5.2. Functional Analysis of 5'UTR Variants

In the second part of this study, four regulatory site variants were used to unravel their effect on expression of *GJB1* gene and to confirm that they can be causative mutations in the respective CMT patients. The investigation was performed using luciferase reporter gene assay protocol. For this purpose, luciferase reporter plasmids that contain 5'UTR sequence of *GJB1* with specific variants were generated by direct cloning or site-directed mutagenesis followed by cloning. When plasmids were successfully constructed, HEK293T cells were co-transfected with various plasmids and the effect of variants on gene expression were investigated.

5.2.1. Construction of Plasmids

DNA fragments of 5'UTR of *GJB1* to be cloned into luciferase vector were amplified by PCR using corresponding patient genomic DNA samples as templates (Figure 5.8). Expected band size was 1028 base pairs. Each fragment generated by PCR carried one of the three variants, namely, c.-18A>G, c.-528T>C, and c.-713G>A. The fourth plasmid was engineered to harbor the wild type 5'UTR sequence.

The *GJB1* promoter variants identified in our laboratory and investigated in this study are given in Table 5.2.

Table 5.2. Patients that used for amplification of insert DNA and corresponding variants.

Variant	**Patient**
c.-18A>G	P158
c.-528T>C	P727
c.-713G>A	P412
Wild-type	P1323

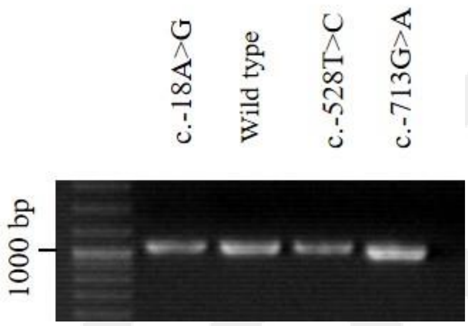

Figure 5.10. Agarose gel image of PCR amplified *GJB1*-5'UTR fragments.

5'UTR fragments of *GJB1* gene were cloned into pGL2-basic luciferase vector by Gibson Assembly reaction as described in section 4.4.5. Subsequently, each plasmid was used to transform competent bacteria. Transformed bacteria were grown in selective LB-agar plates containing 100 µg/ml ampicillin. The other day, five colonies for each variant were selected for colony PCR. Results of colony PCR were given in Figures 5.11 - 5.12.

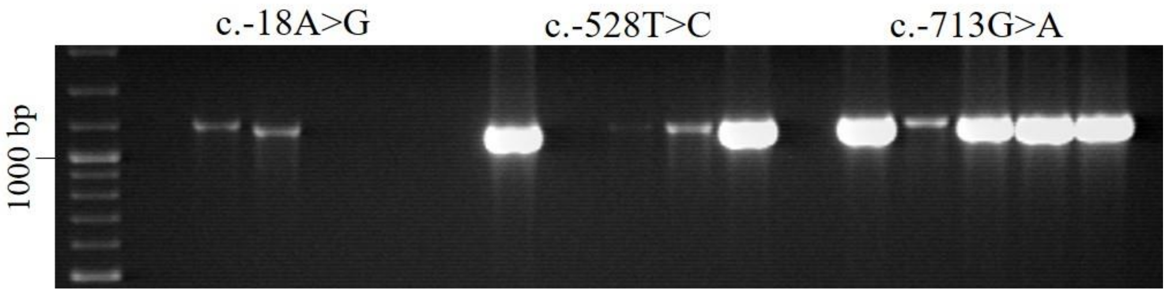

Figure 5.11. Agarose gel image of colony PCR results.

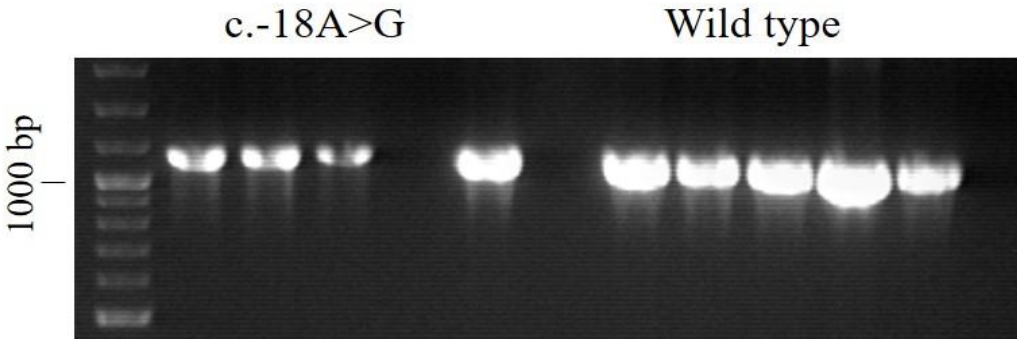

Figure 5.12. Agarose gel image of colony PCR results.

For each colony PCR results, 1100 bp band which contains our insert sequence and several nucleotides from the ends of vector backbone was expected. The variants on each successful PCR product were verified by sequencing and further used for production of overnight bacterial culture.

5.2.2. Purification of Plasmids

Selected colonies were grown in LB medium with 100 μg/ml ampicillin for overnight at 37^{o}C while rotating at 250 rpm. The other day, plasmids were isolated by using High Pure MiniPrep kit or HiPure Maxiprep kit (Figure 5.10).

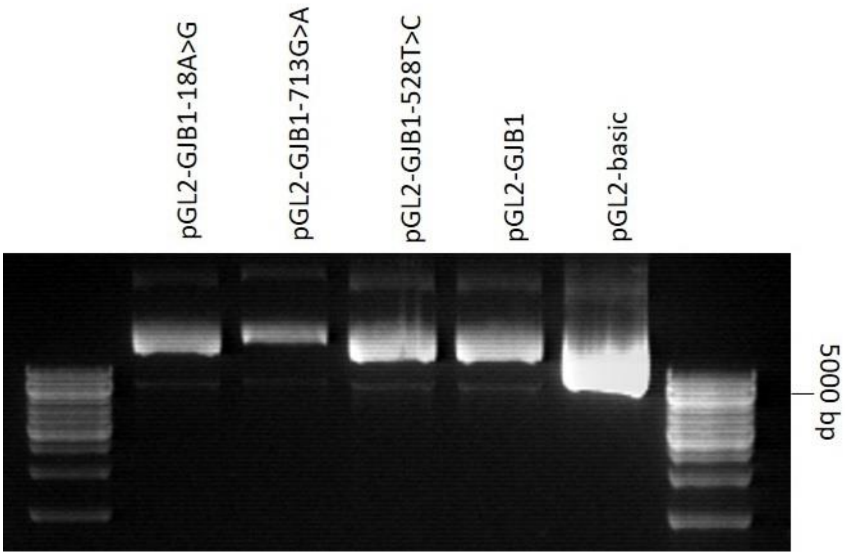

Figure 5.13. Agarose gel image of purified plasmids.

The purified plasmids were stored at -20°C until further use. The map of generated plasmid was given in Figure 5.14.

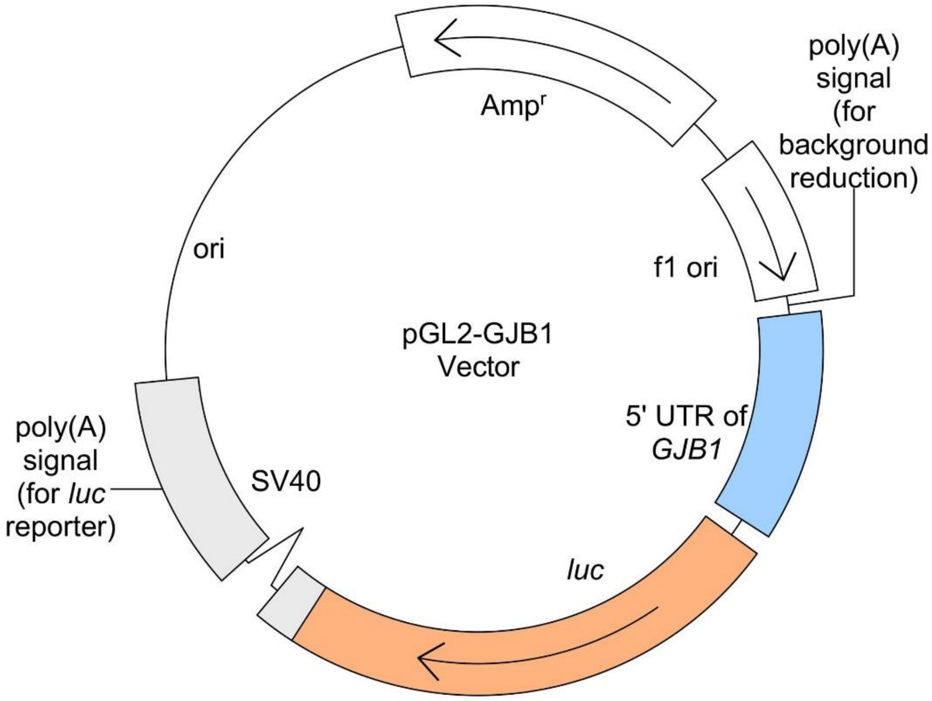

Figure 5.14. The map of pGL2-GJB1 vector.

5.2.3. Generation of c.-541A>G Variant by Site-Directed Mutagenesis

The genomic DNA of the patient who has the c.-541A>G variant was not available, unfortunately. To overcome this problem, this variant was generated by site-directed mutagenesis on the plasmid containing wild type sequence of *GJB1*-5'UTR. First, wild type plasmid was amplified and linearized by PCR using primers containing c.-541A>G variant (Figure 5.15).

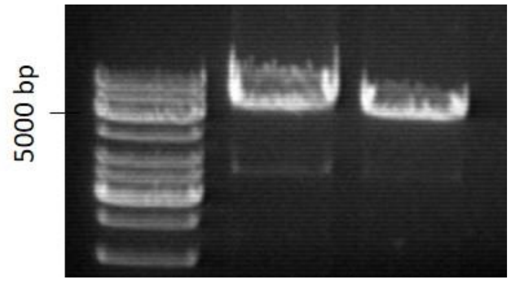

Figure 5.15. Agarose gel image of linearized wild type plasmids by PCR using primers containing c.-541A>G variant.

After ligation of mutated plasmid, the product was subsequently used for bacterial transformation. Transformed bacteria were grown overnight at 37^{o}C. The next day, five colonies were selected and used for colony PCR. Result of colony PCR was shown in Figure 5.16.

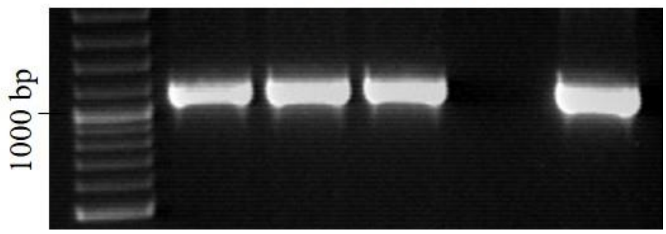

Figure 5.16. Agarose gel image of colony PCR results containing c.-541A>G variant.

According to colony PCR results, successful colonies were selected and used for bacterial culture production. Expected band size was approximately 1100 bp which contains our insert and several nucleotides from the ends of vector backbone. Selected colonies were grown in LB medium that contains 100 µg/ml ampicillin for overnight at 37^{o}C while rotating at 250 rpm. Sixteen hours later, plasmids were isolated by using High Pure MiniPrep kit or HiPure Maxiprep kit (Figure 5.17).

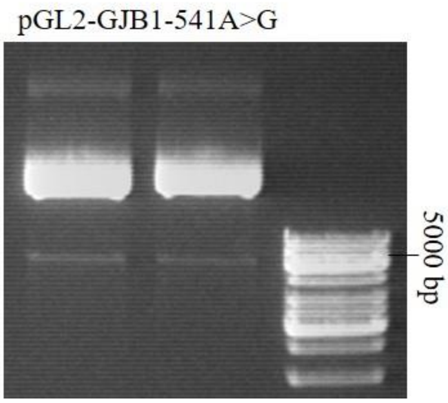

Figure 5.17. Agarose gel image of purified plasmids containing c.-541A>G variant.

5.3. Co-transfection of HEK293T Cells and Luciferase Assay

HEK293T cells were grown in 12-well plates which contains DMEM medium supplemented with 10% FBS at 37°C and 5% CO_2. When cells have reached 80-90% confluency, they were co-transfected with specific plasmids. These plasmids are various pGL2-GJB1 plasmids with/ without specific variants, SOX10 expression plasmid and pRL-SV40 (Renilla Luciferase), internal control plasmid. *GJB1* gene contains two SOX10 transcription factor binding sites on its 5'UTR regulatory region. The expression of *GJB1* gene is known to be initiated upon binding of SOX10 protein to these sites. Because HEK293T cells don't express this protein, SOX10 production was provided by co-transfection of a SOX10 expression plasmid along with other luciferase constructs. On the other hand, a renilla luciferase vector was also used as an internal control in co-transfection to normalize firefly luciferase activity. Normalizing the expression of Firefly luciferase activity reporter to the expression of a control reporter such as Renilla can effectively eliminate nonspecific cellular responses. Firefly and Renilla luciferases are widely used as co-reporters for these normalized studies because both assays are quick, easy and sensitive. Firefly luciferase is a 61kDa and isolated from *Photinus pyralis* while Renilla luciferase a 36kDa protein and isolated from *Renilla reniformis*. Both are monomeric and neither requires post-translational processing, so they can function as genetic reporters immediately upon translation.

Firefly and Renilla luminescence reads for each variant was measured by Luminometer as described in section 4.7. The light emitted from a luciferase reaction is quite broad across many wavelengths. Luminometer collects light from the entire visible spectrum. Therefore, there is no need to filter specific wavelengths for luminescence assays such as luciferase. Relative luciferase activity was calculated as the ratio of firefly luciferase to renilla luciferase. Relative luciferase activities due to various mutations were shown in Figure 5.15. pGL2-GJB1 plasmid that contains wild type sequence was used as a positive control and reference. The pGL2-basic vector, which does not carry any *GJB1* sequence, was shown as a negative control. Data for these experiments are given in Appendix C.

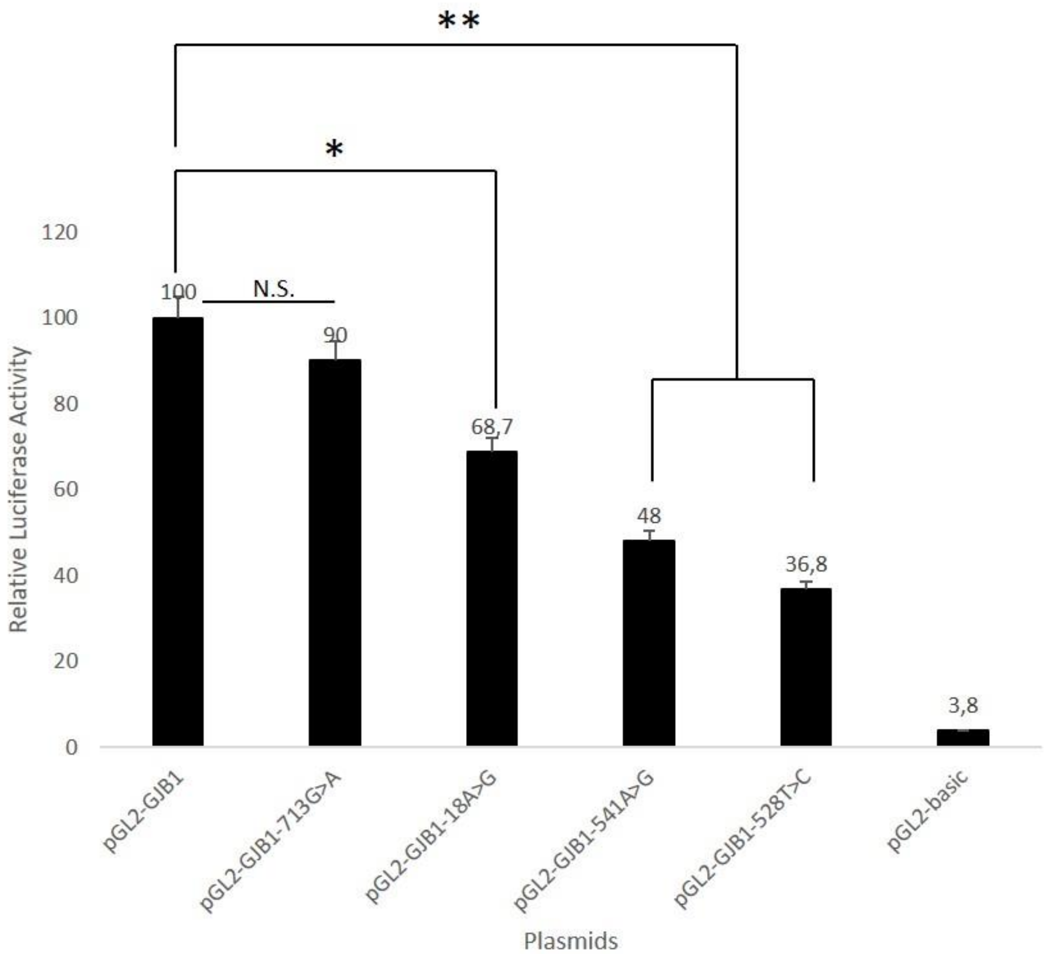

Figure 5.18. Functional impact of the variants in the *GJB1*-5'UTR on luciferase expression and its activity. Error bars represent the standard error of the mean from three independent experiments. * $p < 0.05$; ** $p < 0.01$; N.S. not significant.

According to these results, the previously reported c.-713G>A, did not have any significant effect (10% reduction) on reducing the luciferase activity. The c.-18A>G mutation caused 31% ($p = 0.0124$) decrease in luciferase activity relative to pGL2-GJB1. On the other hand, the c.-541A> G and c.-528T> C mutations that were located on SOX10 binding site of *GJB1* P2 promoter region, significantly reduced gene expression by 52% ($p = 0.0021$) and 63.2% ($p = 0.001$), respectively.

6. DISCUSSION

During this study, 50 patients from our Turkish CMT cohort were investigated for *GJB1* gene mutations. The criteria used for selection of patients include suspected X-linked inheritance in their pedigree and presence of intermediate (30-45m/sec) motor median nerve conduction velocity (MM-NCV). All patients were screened for mutations on 5'UTR of *GJB1* gene. Thirty six of them were also analyzed for coding region mutations. Eight different mutations were identified in the *GJB1* gene; three of them being in 5'UTR of the gene.

In the second part of this study, the effect of four different 5' UTR mutations in the *GJB1* gene was investigated by luciferase reporter gene assay.

6.1. Mutation Analysis of *GJB1*

6.1.1. Mutations on CDS of *GJB1*

Mutations in *GJB1* (Cx32) gene are the second most common cause of CMT after PMP22 duplications (Dubourg *et al.*, 2001). *GJB1* gene mutations that are associated with CMTX1 phenotype is responsible for almost 90% of all CMTX and 10% of all CMT cases (Ressot and Bruzzone, 2000; Scherer, 1996).

Up to now, more than 400 mutations have been described in all regions of *GJB1* (Kleopa *et al* 2012). Most of these mutations are located on protein coding region of the gene and all mutation types (missense, nonsense, deletions, insertions and frameshifts) were observed so far. In this study, 16% of patients (8/50) were found to carry five different mutations in protein coding region of *GJB1* gene. This also validates our criteria while selecting patients for *GJB1* mutations.

First coding region mutation (c.379A>C) was observed in a male patient (P1021), his mother (P1020) and in another male patient (P1186) from a different family. This variant was not found in dbSNP, IPN Mutation and HGMD databases. The c.379A>C variant causes transition of Isoleucine to Leucine at 127th amino acid position (I127L). Both of these amino acids have similar molecular structures, therefore, it may be hypothesized that this variant may not interfere with formation of functional gap junctions. Moreover, the variant affects an amino acid located in the intracellular domain and less likely to cause conformational changes in connexon formation. On the other hand, Isoleucine to Serine change was previously reported at the same position with a different nucleotide change by Vondracek *et al*. in 2005. Clinical findings such as intermediate MM-NCV and distal weakness observed in our affected patients (P1186, P1020 and P1021) were consistent with that of the previously reported I127S phenotype, implicating a possible pathogenic effect. In addition, according to in silico analysis performed by Polyphen2 and MutationTaster software, this variant was predicted as disease causing mutation.

Another mutation (c.43C>T) in CDS of *GJB1* gene was identified in one male (P1113) and one female (P553) patient from different families. The mutation causes replacement of positively charged Arginine with Tryptophan that contains a hydrophobic side chain (R15W). This mutation was previously reported by Janssen *et al*. in 1997. Using voltage clump experiments, Abrams *et al*. in 2001 had shown that it leads to formation of non-functional gap junctions with an unknown mechanism.

The third coding region mutation, c.622G>A, was identified in a male patient (P763). The variant leads to transition of negatively charged Glutamic Acid into positively charged Lysine at amino acid position 208 (E208K). This mutation was first reported by Fairweather *et al*. in 1994 and shown to cause non-functional gap junctions by Wang *et al.* in 2004. In immune-cytochemical analysis using confocal microscopy, it was observed that in E208K mutants Cx32 proteins diffusely distributed in the cytoplasm. This suggests that the mutation prevents the intracellular trafficking of Cx32 from ER-Golgi complex to gap-junction sites and cause the cytoplasmic accumulation of Cx32 without formation of hemi-channels. It is possible that E208K mutation cause Cx32 proteins to be retained in the endoplasmic reticulum and Golgi apparatus (Deschenes *et al*., 1997; Martin *et al*., 2000).

The fourth mutation (c.502T>A) was observed in a male patient (P1027-3) with a severe phenotype. The mutation causes Cysteine to Serine transition at amino acid position 168 (C168S). Although the variant was not reported in dbSNP, IPN Mutation and HGMD databases, two different amino acid changes (C168R; C168Y) were previously reported for the same amino acid position (Choi *et al*. 2004; Paulson *et al*. 2002). Since Cysteine and Serine amino acids have different side chains (-SH; -OH, respectively), this mutation may interfere with the formation of normal 3D structure of the polypeptide. According to clinical examination, affected patient (P1027-3) has a severe phenotype with abnormal mobility, distal weakness, *pes cavus*, intermediate MM-NCV and age of onset (11-20 yrs). Clinical findings support the possibility of pathogenic effect of the mutation. Moreover, in silico algorithms (Polyphen2 and MutationTaster software) predicted this variant as a disease causing mutation. On the other hand, it was reported that patients with C168Y mutations were presenting with CNS myelin dysfunction (Kleopa *et al*. 2005). According to immune-cytochemical analysis, in C168Y mutants Cx32 proteins are retained intracellularly in endoplasmic reticulum and produce no gap junctions (Abrams *et al*. 2017).

The last mutation (c.47A>T) that was identified in CDS of *GJB1* was observed in a female patient (P711). The mutation was previously reported by Keckarevic-Markovic in 2009 and causes alteration of positively charged Histidine to hydrophobic Leucine at 16th amino acid position (H16L). Histidine amino acid has an aromatic side chain that is not present in Leucine. In order to understand how this mutation affects gap junctions further analysis is required.

6.1.2. Mutations in 5’UTR of *GJB1* and Their Effects on Gene Expression

Mutational analysis of 5’UTR of *GJB1* revealed three different variants in 50 patients that were presented in Figure 6.1. Among those variants, c.-713G>A was observed in 25 patients, corresponding to a 50% frequency among our CMT patients. Moreover, three patients (P1020, P763 and P711) that were shown to have a mutation in their coding region were also found to carry this variant in their 5’UTR sequence. This variant was described as a polymorphism in dbSNP and IPN Mutation databases. On the other hand, it was initially reported as regulatory site mutation and shown to reduce gene expression by Wang *et al*. in 2000. However, they performed reporter gene assays in CHO cells that lacks transcription factor SOX10 expression. Since SOX10 activation in P2 promoter site is required for *GJB1* gene expression, c.-713G>A was analyzed again in our functional assays (Figure 6.1). According to relative luciferase activities (Figure 5.18), the variant did not cause a significant decrease (10%) in the *GJB1* gene expression compared to control sample. In patients with this variant, the onset age was usually between 11 and 20 and they had relatively high MM - NCV values (40-50 m/sec). Interestingly, several of these patients presented vocal cord paralysis and moderate severity. In the light of these findings it can be suggested that this variant might have a cumulative effect with other polymorphisms or variants even on different genes (such vocal cord related genes) that leads to development of neuropathy.

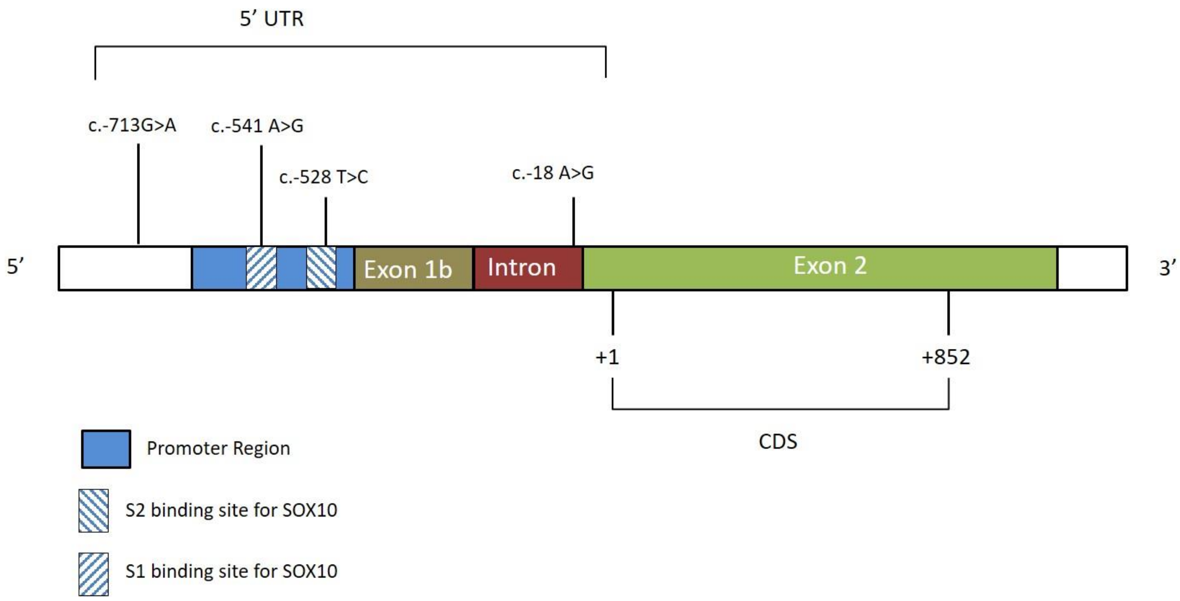

Figure 6.1. Diagram of *GJB1* and upstream mutations that were investigated in this study.

The c.-257C>T variant was identified in a female patient (P374) and described as a polymorphism on dbSNP, 1000 Genome and HapMap databases. In addition, the patient who carry this polymorphism was found positive for c.-713G>A variant that was also described as a polymorphism. Further analysis is required for these two variants to determine whether they have a cumulative effect on development of neuropathy.

The third variant (c.-18A>G) in the 5'UTR of *GJB1* was identified in two male patients (P980 and P1256). It was also was shown to segregate with the disease phenotype in family P158 in our lab's previous studies (Erdoğan, 2012) (Figure 1.7). The effect of this variant on *GJB1* expression was also investigated by luciferase reporter gene assays. The c.-

18A>G variant was shown to cause a statistically significant decrease in the expression of *GJB1* gene (31.3% reduction) compared to the wild type sample. P2 promoter mediated transcription of *GJB1* gene starts from exon 1b and contains 357 bp intron and exon 2 that contains the ORF (Figures B.1). After transcription, exon 1b and intron is spliced out by RNA splicing, leaving only exon 2 in the final transcript. The variant identified in this study is located in close proximity to intron and exon 2 junction and it was predicted as a splice site mutation by in silico analysis (Human Splicing Finder software). According to this analysis, c.-18A>G causes 32.97% disruption in the splicing acceptor motif (GGTGTTTTGCAGGT) recognized by SRP40 (Figure 6.2). This prediction is consistent with our reporter gene assay in which c.-18A>G variant caused 31.3% reduction in luciferase expression. In addition, in silico analysis also revealed that same variant also generates a new motif (GTTTTGCG) that is predicted to be an exonic splicing silencer (ESS) site recognized by SC35 protein (Figure 6.3). In the light of these predictions, it can be suggested that c.-18A>G mutation disrupts splicing in about 30 per cent of the *GJB1* transcripts and leads to inclusion of exon 1b and intron in the mature transcript that ultimately cause production of an abnormal protein. In this case, such transcripts contain pre-mature stop codons and result in truncated protein or degraded by nonsense-mediated decay (NMD).

Splice site type	Motif	New splice site	Wild Type	Mutant	Variation (%)
Acceptor	GGTGTTTTGCAGGT	ggtgttttgcggGT	87.77	58.83	Site broken -32.97

Figure 6.2. In silico analysis of c.-18A>G.

Linked SR protein	Reference Motif (value 0-100)	Linked SR protein	Mutant Motif (value 0-100)	Variation
		SC35	GTTTTGCG (76.89)	New site
SRp40	TTGCAGG (82.51)			Site broken -100

Figure 6.3. Generated splice site motif.

Two variants (c.-541A>G and c.-528T>C) that located on the SOX10 binding sites of *GJB1* promoter region were previously identified in our lab (Erdoğan, 2012). These variants are not found in dbSNP, IPN Mutation and HGMD databases and it can be predicted that they might significantly reduce *GJB1* gene expression as interfering the binding of the

SOX10 transcription factor to the P2 promoter region (Figure 6.1). In order to determine their effects on *GJB1* gene expression, luciferase reporter gene assay was performed. According to relative luciferase activities, it was observed that c.-541A>G and c.-528T>C variants cause statistically significant decrease (52% and 63.2%, respectively) in expression of *GJB1* gene (Figure 5.18). This findings suggests that these two mutations are responsible for the CMTX1 phenotype. Clinical analysis of patients with these mutations also showed that the NCV values of patients were between 27-40 m/sec which is consistent with the typical CMTX1 phenotype.

7. CONCLUSION

This study contributed to molecular diagnosis of CMTX1 with identification of five different mutations including two novel mutations (p.Ile127Leu and p.Cys168Ser) in coding region of *GJB1*. We also described a common upstream variant (c.-713G>A) in our CMT population. In addition, three novel upstream variants (c.-18A>G, c.-541A>G and c.-528T>C) identified in our lab were shown to reduce the level of gene expression, implicating significance of upstream mutations for CMTX1 genetic diagnosis.

REFERENCES

Abrams, C. K., M. V. Bennett, V. K. Verselis and T. A. Bargiello. "Voltage Opens Unopposed Gap Junction Hemichannels Formed by a Connexin 32 Mutant Associated with X-Linked Charcot-Marie-Tooth Disease." *Proc Natl Acad Sci U S A* 99, no. 6 (2002): 3980-4.

Abrams, C. K. and M. Freidin. "Gjb1-Associated X-Linked Charcot-Marie-Tooth Disease, a Disorder Affecting the Central and Peripheral Nervous Systems." *Cell Tissue Res* 360, no. 3 (2015): 659-73.

Abrams, C. K., M. M. Freidin, V. K. Verselis, M. V. Bennett and T. A. Bargiello. "Functional Alterations in Gap Junction Channels Formed by Mutant Forms of Connexin 32: Evidence for Loss of Function as a Pathogenic Mechanism in the X-Linked Form of Charcot-Marie-Tooth Disease." *Brain Res* 900, no. 1 (2001): 9-25.

Appu, M. and S. Mar. "Novel Familial Pathogenic Mutation in Gap Junction Protein, Beta-1 Gene (Gjb1) Associated with Transient Neurological Deficits in a Patient with X-Linked Charcot-Marie-Tooth Disease." *Muscle Nerve* 50, no. 6 (2014): 1023-4.

Arthur-Farraj, P. J., S. M. Murphy, M. Laura, M. P. Lunn, H. Manji, J. Blake, G. Ramdharry, Z. Fox and M. M. Reilly. "Hand Weakness in Charcot-Marie-Tooth Disease 1x." *Neuromuscul Disord* 22, no. 7 (2012): 622-6.

Bahr, M., F. Andres, V. Timmerman, M. E. Nelis, C. Van Broeckhoven and J. Dichgans. "Central Visual, Acoustic, and Motor Pathway Involvement in a Charcot-Marie-Tooth Family with an Asn205ser Mutation in the Connexin 32 Gene." *J Neurol Neurosurg Psychiatry* 66, no. 2 (1999): 202-6.

Berciano, J. "Peripheral Neuropathies: Molecular Diagnosis of Charcot-Marie-Tooth Disease." *Nat Rev Neurol* 7, no. 6 (2011): 305-6.

Bergamin, G., F. Boaretto, C. Briani, E. Pegoraro, M. Cacciavillani, A. Martinuzzi, M.

Muglia, A. Vettori, G. Vazza and M. L. Mostacciuolo. "Mutation Analysis of Mfn2, Gjb1, Mpz and Pmp22 in Italian Patients with Axonal Charcot-Marie-Tooth Disease." *Neuromolecular Med* 16, no. 3 (2014): 540-50.

Bergmann, C., J. M. Schroder, S. Rudnik-Schoneborn, K. Zerres and J. Senderek. "A Point Mutation in the Human Connexin32 Promoter P2 Does Not Correlate with X-Linked Dominant Charcot-Marie-Tooth Neuropathy in Germany." *Brain Res Mol Brain Res* 88, no. 1-2 (2001): 183-5.

Bondurand, N., M. Girard, V. Pingault, N. Lemort, O. Dubourg and M. Goossens. "Human Connexin 32, a Gap Junction Protein Altered in the X-Linked Form of Charcot-Marie-Tooth Disease, Is Directly Regulated by the Transcription Factor Sox10." *Hum Mol Genet* 10, no. 24 (2001): 2783-95.

Choi, B. O., M. S. Lee, S. H. Shin, J. H. Hwang, K. G. Choi, W. K. Kim, I. N. Sunwoo, N. K. Kim and K. W. Chung. "Mutational Analysis of Pmp22, Mpz, Gjb1, Egr2 and Nefl in Korean Charcot-Marie-Tooth Neuropathy Patients." *Hum Mutat* 24, no. 2 (2004): 185-6.

Fairweather, N., C. Bell, S. Cochrane, J. Chelly, S. Wang, M. L. Mostacciuolo, A. P. Monaco and N. E. Haites. "Mutations in the Connexin 32 Gene in X-Linked Dominant Charcot-Marie-Tooth Disease (Cmtx1)." *Hum Mol Genet* 3, no. 1 (1994): 29-34.

Flagiello, L., V. Cirigliano, M. Strazzullo, V. Cappa, A. Ciccodicola, M. D'Esposito, I. Torrente, R. Werner, G. Di Iorio, M. Rinaldi, A. Dallapiccola, A. Forabosco, V. Ventruto and M. D'Urso. "Mutation in the Nerve-Specific 5'non-Coding Region of Cx32 Gene and Absence of Specific Mrna in a Cmtx1 Italian Family. Mutations in Brief No. 195. Online." *Hum Mutat* 12, no. 5 (1998): 361.

Goldberg, G. S., V. Valiunas and P. R. Brink. "Selective Permeability of Gap Junction Channels." *Biochim Biophys Acta* 1662, no. 1-2 (2004): 96-101.

Guo, F., Y. Shi, Y. Lin, X. Liu, B. Liu, Y. Liu, Y. Yang, F. Lu, S. Ma and Z. Yang. "Mutation in Connexin 32 Causes Charcot-Marie-Tooth Disease in a Large Chinese Family." *Muscle Nerve* 42, no. 5 (2010): 715-21.

Hahn, A. F., P. J. Ainsworth, C. C. Naus, J. Mao and C. F. Bolton. "Clinical and Pathological Observations in Men Lacking the Gap Junction Protein Connexin 32." *Muscle Nerve Suppl* 9, (2000): S39-48.

Houlden, H., M. Girard, C. Cockerell, D. Ingram, N. W. Wood, M. Goossens, R. W. Walker and M. M. Reilly. "Connexin 32 Promoter P2 Mutations: A Mechanism of Peripheral Nerve Dysfunction." *Ann Neurol* 56, no. 5 (2004): 730-4.

Human Splicing Finder. http://www.umd.be/HSF3/, accessed at April, 2017.

Ionasescu, V. V., C. Searby, R. Ionasescu, I. M. Neuhaus and R. Werner. "Mutations of the Noncoding Region of the Connexin32 Gene in X-Linked Dominant Charcot-Marie-Tooth Neuropathy." *Neurology* 47, no. 2 (1996): 541-4.

Janssen, E. A., S. Kemp, G. W. Hensels, O. G. Sie, C. E. de Die-Smulders, J. E. Hoogendijk, M. de Visser and P. A. Bolhuis. "Connexin32 Gene Mutations in X-Linked Dominant Charcot-Marie-Tooth Disease (Cmtx1)." *Hum Genet* 99, no. 4 (1997): 501-5.

JM, U. King-Im, E. Yiu, E. J. Donner and M. Shroff. "Mri Findings in X-Linked Charcot-Marie-Tooth Disease Associated with a Novel Connexin 32 Mutation." *Clin Radiol* 66, no. 5 (2011): 471-4.

Karadima, G., G. Koutsis, M. Raftopoulou, P. Floroskufi, K. M. Karletidi and M. Panas. "Four Novel Connexin 32 Mutations in X-Linked Charcot-Marie-Tooth Disease. Phenotypic Variability and Central Nervous System Involvement." *J Neurol Sci* 341, no. 1-2 (2014): 158-61.

Keckarevic-Markovic, M., V. Milic-Rasic, J. Mladenovic, J. Dackovic, M. Kecmanovic, D. Keckarevic, D. Savic-Pavicevic and S. Romac. "Mutational Analysis of Gjb1, Mpz, Pmp22, Egr2, and Litaf/Simple in Serbian Charcot-Marie-Tooth Patients." *J Peripher*

Nerv Syst 14, no. 2 (2009): 125-36.

Kim, Y., K. G. Choi, K. D. Park, K. S. Lee, K. W. Chung and B. O. Choi. "X-Linked Dominant Charcot-Marie-Tooth Disease with Connexin 32 (Cx32) Mutations in Koreans." *Clin Genet* 81, no. 2 (2012): 142-9.

Kleopa, K. A. "The Role of Gap Junctions in Charcot-Marie-Tooth Disease." *J Neurosci* 31, no. 49 (2011): 17753-60.

Kleopa, K. A., C. K. Abrams and S. S. Scherer. "How Do Mutations in Gjb1 Cause X-Linked Charcot-Marie-Tooth Disease?" *Brain Res* 1487, (2012): 198-205.

Kleopa, K. A. and S. S. Scherer. "Inherited Neuropathies." *Neurol Clin* 20, no. 3 (2002): 679-709.

Koval, M. "Pathways and Control of Connexin Oligomerization." *Trends Cell Biol* 16, no. 3 (2006): 159-66.

Kuhlbrodt, K., B. Herbarth, E. Sock, I. Hermans-Borgmeyer and M. Wegner. "Sox10, a Novel Transcriptional Modulator in Glial Cells." *J Neurosci* 18, no. 1 (1998): 237-50.

Kumar, N. M. and N. B. Gilula. "Cloning and Characterization of Human and Rat Liver Cdnas Coding for a Gap Junction Protein." *J Cell Biol* 103, no. 3 (1986): 767-76.

Kuntzer, T., M. Dunand, D. F. Schorderet, J. M. Vallat, A. F. Hahn and J. Bogousslavsky. "Phenotypic Expression of a Pro 87 to Leu Mutation in the Connexin 32 Gene in a Large Swiss Family with Charcot-Marie-Tooth Neuropathy." *J Neurol Sci* 207, no. 1-2 (2003): 77-86.

Li, Q., M. Chen, K. Liu, X. Lin and D. Chui. "Vocal Cord Paresis and Probable X-Linked Charcot-Marie-Tooth Disease with Novel Gjb1 Mutation." *Int J Neurosci* 120, no. 11 (2010): 731-4.

Li, Q. H., K. X. Liu, J. L. Feng, A. Y. Zeng, H. Li, L. Wu, Y. G. Tang, M. L. Chen, X. H. Lin and J. Z. Jiang. "[a New Mutation in the Gjb1 Gene of a Chinese Family with Charcot-Marie-Tooth Disease Associated with Vocal Cord Paresis]." *Zhonghua Yi Xue Yi Chuan Xue Za Zhi* 27, no. 5 (2010): 497-500.

Liang, G. S., M. de Miguel, J. M. Gomez-Hernandez, J. D. Glass, S. S. Scherer, M. Mintz, L. C. Barrio and K. H. Fischbeck. "Severe Neuropathy with Leaky Connexin32 Hemichannels." *Ann Neurol* 57, no. 5 (2005): 749-54.

Lin, P., F. Mao, Q. Liu, W. Yang, C. Shao, C. Yan and Y. Gong. "A Novel Deletion Mutation in Gjb1 Causes X-Linked Charcot-Marie-Tooth Disease in a Han Chinese Family." *Muscle Nerve* 42, no. 6 (2010): 922-6.

Luigetti, M., G. M. Fabrizi, F. Ranieri, F. Taioli, A. Conte, A. Del Grande and M. Sabatelli. "A Novel Gjb1 Mutation in an Italian Patient with Charcot-Marie-Tooth Disease and Pyramidal Signs." *Muscle Nerve* 44, no. 4 (2011): 613-5.

Martikainen, M. H. and K. Majamaa. "Novel Gjb1 Mutation Causing Adult-Onset Charcot-Marie-Tooth Disease in a Female Patient." *Neuromuscul Disord* 23, no. 11 (2013): 899-901.

Milley, G. M., E. T. Varga, Z. Grosz, B. Bereznai, Z. Aranyi, J. Boczan, P. Dioszeghy, B. Kalman, A. Gal and M. J. Molnar. "Three Novel Mutations and Genetic Epidemiology Analysis of the Gap Junction Beta 1 (Gjb1) Gene among Hungarian Charcot-Marie-Tooth Disease Patients." *Neuromuscul Disord* 26, no. 10 (2016): 706-711.

Mladenovic, J., V. Milic Rasic, M. Keckarevic Markovic, S. Romac, S. Todorovic, V. Rakocevic Stojanovic, D. Kisic Tepavcevic, A. Hofman and T. Pekmezovic. "Epidemiology of Charcot-Marie-Tooth Disease in the Population of Belgrade, Serbia." *Neuroepidemiology* 36, no. 3 (2011): 177-82.

Murphy, S. M., R. Ovens, J. Polke, C. E. Siskind, M. Laura, K. Bull, G. Ramdharry, H. Houlden, R. P. Murphy, M. E. Shy and M. M. Reilly. "X Inactivation in Females with

X-Linked Charcot-Marie-Tooth Disease." *Neuromuscul Disord* 22, no. 7 (2012): 617-21.

Murphy, S. M., J. Polke, H. Manji, J. Blake, L. Reiniger, M. Sweeney, H. Houlden, S. Brandner and M. M. Reilly. "A Novel Mutation in the Nerve-Specific 5'utr of the Gjb1 Gene Causes X-Linked Charcot-Marie-Tooth Disease." *J Peripher Nerv Syst* 16, no. 1 (2011): 65-70.

MutationTaster. http://www.mutationtaster.org/, accessed at April, 2017.

Neuhaus, I. M., G. Dahl and R. Werner. "Use of Alternate Promoters for Tissue-Specific Expression of the Gene Coding for Connexin32." *Gene* 158, no. 2 (1995): 257-62.

Neuromuscular Disease Center. http://neuromuscular.wustl.edu/, accessed at April, 2017.

Nicholson, G. A., L. Yeung and A. Corbett. "Efficient Neurophysiologic Selection of X-Linked Charcot-Marie-Tooth Families: Ten Novel Mutations." *Neurology* 51, no. 5 (1998): 1412-6.

Nicolaou, P., E. Zamba-Papanicolaou, P. Koutsou, K. A. Kleopa, A. Georghiou, G. Hadjigeorgiou, A. Papadimitriou, T. Kyriakides and K. Christodoulou. "Charcot-Marie-Tooth Disease in Cyprus: Epidemiological, Clinical and Genetic Characteristics." *Neuroepidemiology* 35, no. 3 (2010): 171-7.

Oh, S., Y. Ri, M. V. Bennett, E. B. Trexler, V. K. Verselis and T. A. Bargiello. "Changes in Permeability Caused by Connexin 32 Mutations Underlie X-Linked Charcot-Marie-Tooth Disease." *Neuron* 19, no. 4 (1997): 927-38.

Orthmann-Murphy, J. L., M. Freidin, E. Fischer, S. S. Scherer and C. K. Abrams. "Two Distinct Heterotypic Channels Mediate Gap Junction Coupling between Astrocyte and Oligodendrocyte Connexins." *J Neurosci* 27, no. 51 (2007): 13949-57.

Paulson, H. L., J. Y. Garbern, T. F. Hoban, K. M. Krajewski, R. A. Lewis, K. H. Fischbeck, R. I. Grossman, R. Lenkinski, J. A. Kamholz and M. E. Shy. "Transient Central

Nervous System White Matter Abnormality in X-Linked Charcot-Marie-Tooth Disease." *Ann Neurol* 52, no. 4 (2002): 429-34.

Pfenniger, A., A. Wohlwend and B. R. Kwak. "Mutations in Connexin Genes and Disease." *Eur J Clin Invest* 41, no. 1 (2011): 103-16.

Polyphen-2. http://genetics.bwh.harvard.edu/pph2/, accessed at April, 2017.

Qiao, X. H., Y. X. Li, X. Z. Chang, X. H. Luan, B. Chen, D. F. Bu and Y. Yuan. "[Two Novel Mutations of Gjb1 Gene Associated with Typical X-Linked Charcot-Marie-Tooth Disease]." *Zhonghua Yi Xue Za Zhi* 89, no. 47 (2009): 3328-31.

Reilly, M. M., S. M. Murphy and M. Laura. "Charcot-Marie-Tooth Disease." *J Peripher Nerv Syst* 16, no. 1 (2011): 1-14.

Sakaguchi, H., S. Yamashita, A. Miura, T. Hirahara, E. Kimura, Y. Maeda, T. Terasaki, T. Hirano and M. Uchino. "A Novel Gjb1 Frameshift Mutation Produces a Transient Cns Symptom of X-Linked Charcot-Marie-Tooth Disease." *J Neurol* 258, no. 2 (2011): 284-90.

Saporta, A. S., S. L. Sottile, L. J. Miller, S. M. Feely, C. E. Siskind and M. E. Shy. "Charcot-Marie-Tooth Disease Subtypes and Genetic Testing Strategies." *Ann Neurol* 69, no. 1 (2011): 22-33.

Sargiannidou, I., A. Kagiava, S. Bashiardes, J. Richter, C. Christodoulou, S. S. Scherer and K. A. Kleopa. "Intraneural Gjb1 Gene Delivery Improves Nerve Pathology in a Model of X-Linked Charcot-Marie-Tooth Disease." *Ann Neurol* 78, no. 2 (2015): 303-16.

Scherer, S. S. and K. A. Kleopa. "X-Linked Charcot-Marie-Tooth Disease." *J Peripher Nerv Syst* 17 Suppl 3, (2012): 9-13.

Scherer, S. S., Y. T. Xu, A. Messing, K. Willecke, K. H. Fischbeck and L. J. Jeng. "Transgenic Expression of Human Connexin32 in Myelinating Schwann Cells Prevents

Demyelination in Connexin32-Null Mice." *J Neurosci* 25, no. 6 (2005): 1550-9.

Segretain, D. and M. M. Falk. "Regulation of Connexin Biosynthesis, Assembly, Gap Junction Formation, and Removal." *Biochim Biophys Acta* 1662, no. 1-2 (2004): 3-21.

Senderek, J., B. Hermanns, C. Bergmann, B. Boroojerdi, M. Bajbouj, M. Hungs, V. T. Ramaekers, S. Quasthoff, D. Karch and J. M. Schroder. "X-Linked Dominant Charcot-Marie-Tooth Neuropathy: Clinical, Electrophysiological, and Morphological Phenotype in Four Families with Different Connexin32 Mutations(1)." *J Neurol Sci* 167, no. 2 (1999): 90-101.

Shy, M. E., C. Siskind, E. R. Swan, K. M. Krajewski, T. Doherty, D. R. Fuerst, P. J. Ainsworth, R. A. Lewis, S. S. Scherer and A. F. Hahn. "Cmt1x Phenotypes Represent Loss of Gjb1 Gene Function." *Neurology* 68, no. 11 (2007): 849-55.

Siskind, C. E., S. Panchal, C. O. Smith, S. M. Feely, J. C. Dalton, A. B. Schindler and K. M. Krajewski. "A Review of Genetic Counseling for Charcot Marie Tooth Disease (Cmt)." *J Genet Couns* 22, no. 4 (2013): 422-36.

Sohl, G., C. Gillen, F. Bosse, M. Gleichmann, H. W. Muller and K. Willecke. "A Second Alternative Transcript of the Gap Junction Gene Connexin32 Is Expressed in Murine Schwann Cells and Modulated in Injured Sciatic Nerve." *Eur J Cell Biol* 69, no. 3 (1996): 267-75.

Sohl, G., P. A. Nielsen, J. Eiberger and K. Willecke. "Expression Profiles of the Novel Human Connexin Genes Hcx30.2, Hcx40.1, and Hcx62 Differ from Their Putative Mouse Orthologues." *Cell Commun Adhes* 10, no. 1 (2003): 27-36.

Sohl, G., M. Theis, G. Hallas, S. Brambach, E. Dahl, G. Kidder and K. Willecke. "A New Alternatively Spliced Transcript of the Mouse Connexin32 Gene Is Expressed in Embryonic Stem Cells, Oocytes, and Liver." *Exp Cell Res* 266, no. 1 (2001): 177-86.

Tsai, P. C., C. H. Chen, A. B. Liu, Y. C. Chen, B. W. Soong, K. P. Lin, S. F. Yet and Y. C.

Lee. "Mutational Analysis of the 5' Non-Coding Region of Gjb1 in a Taiwanese Cohort with Charcot-Marie-Tooth Neuropathy." *J Neurol Sci* 332, no. 1-2 (2013): 51-5.

Vondracek, P., P. Seeman, M. Hermanova and L. Fajkusova. "X-Linked Charcot-Marie-Tooth Disease: Phenotypic Expression of a Novel Mutation Ile127ser in the Gjb1 (Connexin 32) Gene." *Muscle Nerve* 31, no. 2 (2005): 252-5.

Vrancken, A. F., W. G. Spliet and F. van Ruissen. "X-Linked Charcot-Marie-Tooth Disease with Novel C.47a>T Gjb1 Gene Mutation." *J Peripher Nerv Syst* 15, no. 2 (2010): 156-7.

Wang, H. L., W. T. Chang, T. H. Yeh, T. Wu, M. S. Chen and C. Y. Wu. "Functional Analysis of Connexin-32 Mutants Associated with X-Linked Dominant Charcot-Marie-Tooth Disease." *Neurobiol Dis* 15, no. 2 (2004): 361-70.

Wang, H. L., T. Wu, W. T. Chang, A. H. Li, M. S. Chen, C. Y. Wu and W. Fang. "Point Mutation Associated with X-Linked Dominant Charcot-Marie-Tooth Disease Impairs the P2 Promoter Activity of Human Connexin-32 Gene." *Brain Res Mol Brain Res* 78, no. 1-2 (2000): 146-53.

Wu, T., H. L. Wang, C. C. Chu, J. M. Yu, J. Y. Chen and C. C. Huang. "Clinical and Electrophysiological Studies of a Family with Probable X-Linked Dominant Charcot-Marie-Tooth Neuropathy and Ptosis." *Chang Gung Med J* 27, no. 7 (2004): 489-500.

Xiao, F., J. Z. Tan, X. Zhang and X. F. Wang. "A Novel Mutation in Gjb1 (C.212t>G) in a Chinese Family with X-Linked Charcot-Marie-Tooth Disease." *J Clin Neurosci* 22, no. 3 (2015): 513-8.

APPENDIX A: PLASMID MAPS

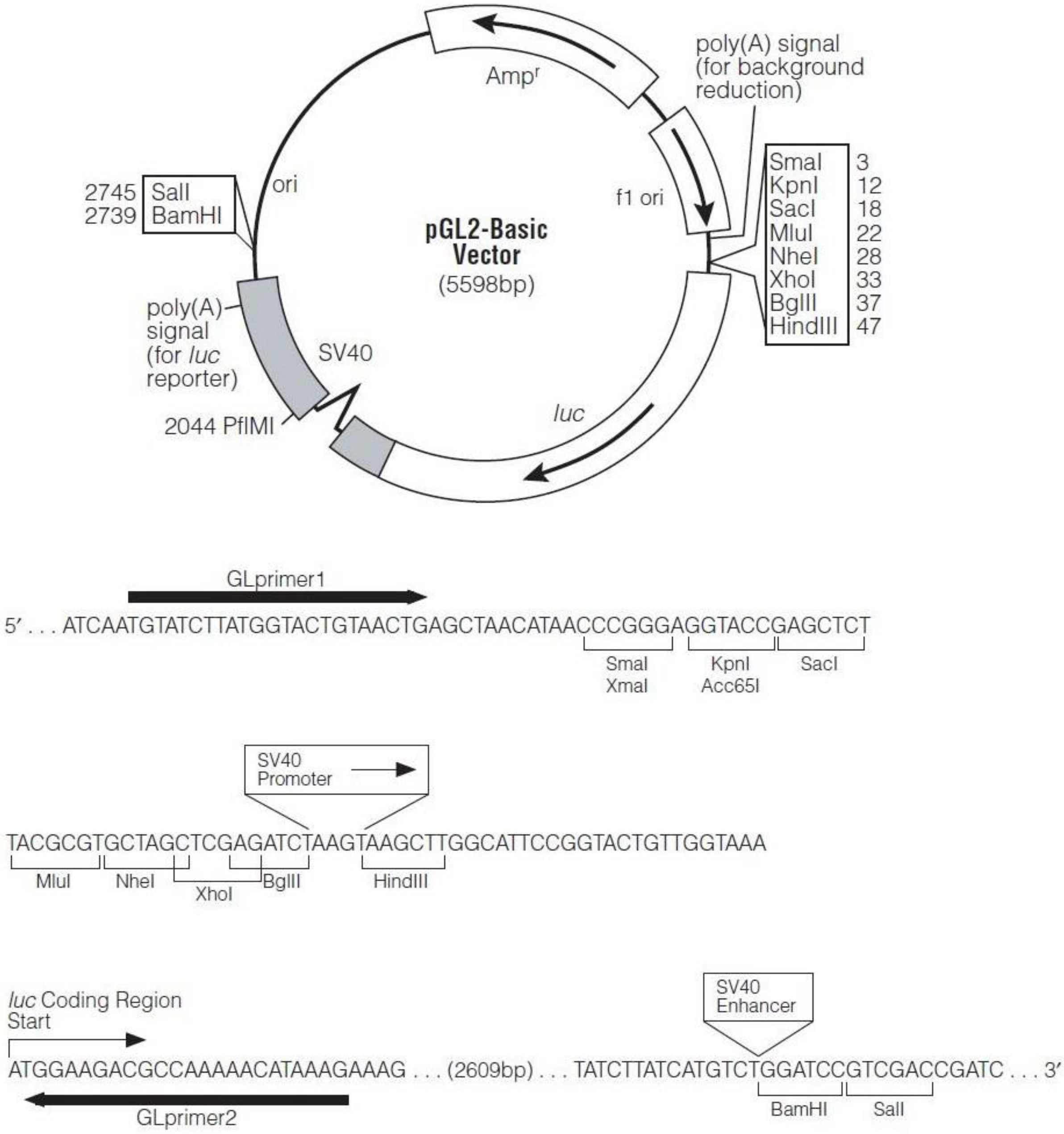

Figure A.1. Restriction map and Multiple Cloning Site (MCS) of pGL2-basic vector which is used to generate pGL2-GJB1 plasmid.

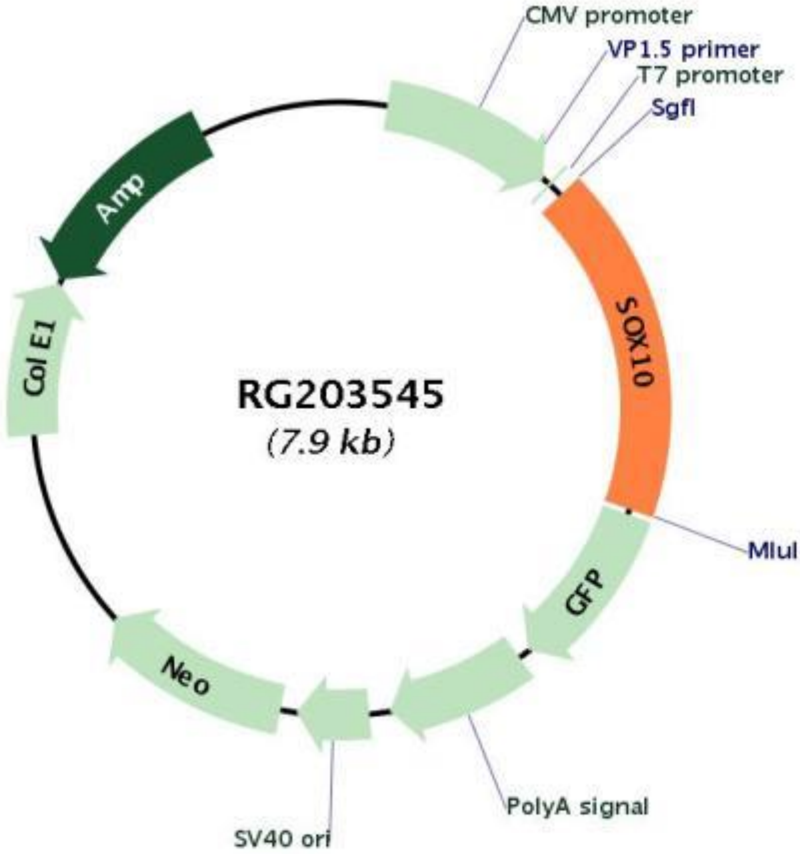

Figure A.2. Map of SOX10 expression plasmid used to provide SOX10 transcription factor protein in HEK293T cells.

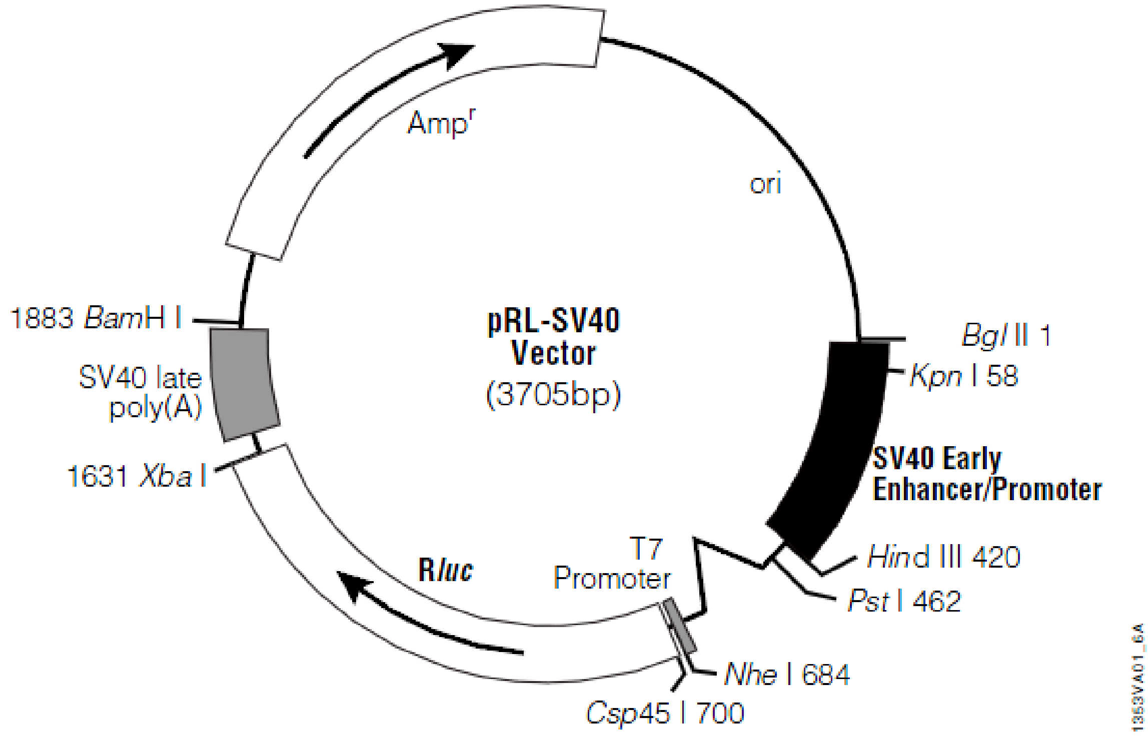

Figure A.3. Map of pRL-SV40 Renilla Luciferase plasmid that used as internal control in luciferase assays.

APPENDIX B: MAP OF SPLICE SITE SEQUENCES

Transcription
Initiation

EXON 1B

CTGGTGGCATAGGGCAGACACGCCTGCAGACATTCTCTGGGAAAGGGCAGCAGCAGCCAGG

c.-18A>G

INTRON

TGTGGCAGTGACAGGGAGgtgaggagactgggggctgagggag..........ttgcttcatggctggtgttttgcagGTGTGAATG

+ 1

EXON 2

AGGCAGGATGAACTGGACAGGTTTGTACACCTTGCTCAGTGGCGTGAACCGGCATTCTACTG
CCATTGGCCGAGTATGGCTCTCGGTCATCTTCATCTTCAGAATCATGGTGCTGGTGGTGGCTG
CAGAGAGTGTGTGGGGTGATGAGAAATCTTCCTTCATCTGCAAC……..........AAAGAGCGACCG
CTGCTCGGCCTGCTGA

Figure B.1. Transcription template sequence and splice site region of *GJB1*.

Transcription
Initiation

EXON 1B

CTGGTGGCATAGGGCAGACACGCCTGCAGACATTCTCTGGGAAAGGGCAGCAGCAGCCAGG

c.-18A>G

INTRON

TGTGGCAGTGACAGGGAGgtgaggagactgggggctgagggag..........ttgcttcatggctggtgttttgcagGTGTGAATG

+ 1

LUCIFERASE

AGGCAGGATGAACTGGACAGATGGAAGACGCCAAAAACATAAAGAAAGGCCCGGCGCCATT
CTATCCTCTAGAGGATGGAACCGCTGGAGAGCAACTGCATAAGG………TTCAGCGATGACG
AAATTCTTAGCTATTGTAATACTGCGATGAGTGGCAGGGCG

Figure B.2. Splice site region of luciferase plasmid containing upstream sequence of *GJB1*.

APPENDIX C: LUCIFERASE ASSAY DATA

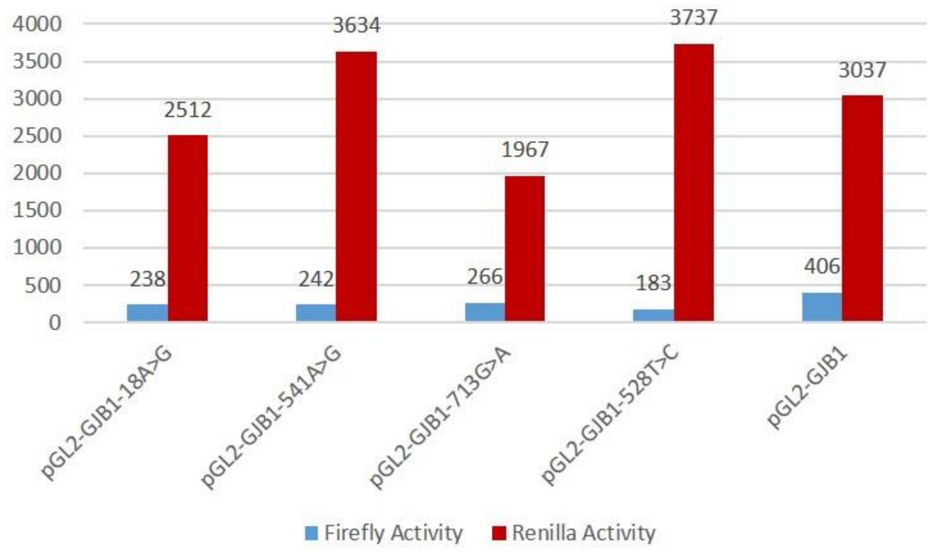

Figure C.1. Signals for firefly and renilla luciferase luminescence for different variants.